Eur. Phys. J. C (2025) 85:927
https://doi.org/10.1140/epjc/s10052-025-14409-1

THE EUROPEAN PHYSICAL JOURNAL C

Regular Article - Experimental Physics

A precise measurement of the jet energy scale derived from single-particle measurements and in situ techniques in proton–proton collisions at $\sqrt{s} = 13$ TeV with the ATLAS detector

ATLAS Collaboration[⋆]

CERN ,1211 Geneva 23, Switzerland

Received: 23 July 2024 / Accepted: 9 June 2025

Abstract The jet energy calibration and its uncertainties are derived from measurements of the calorimeter response to single particles in both data and Monte Carlo simulation using proton–proton collisions at $\sqrt{s} = 13$ TeV collected with the ATLAS detector during Run 2 at the Large Hadron Collider. The jet calibration uncertainty for anti-k_T jets with a jet radius parameter of $R_{\text{jet}} = 0.4$ and in the central jet rapidity region is about 2.5% for transverse momenta (p_{T}) of 20 GeV, about 0.5% for $p_{\text{T}} = 300$ GeV and 0.7% for $p_{\text{T}} = 4$ TeV. Excellent agreement is found with earlier determinations obtained from p_{T}-balance based in situ methods (Z/γ+jets). The combination of these two independent methods results in the most precise jet energy measurement achieved so far with the ATLAS detector with a relative uncertainty of 0.3% at $p_{\text{T}} = 300$ GeV and 0.6% at 4 TeV. The jet energy calibration is also derived with the single-particle calorimeter response measurements separately for quark- and gluon-induced jets and furthermore for jets with R_{jet} varying from 0.2 to 1.0 retaining the correlations between these measurements. Differences between inclusive jets and jets from boosted top-quark decays, with and without grooming the soft jet constituents, are also studied.

1 Introduction

Jets, collimated sprays of hadrons, are ubiquitously produced in proton–proton (pp) collisions at the Large Hadron collider (LHC). In the theory of the strong interaction, Quantum Chromodynamics (QCD), they are interpreted as the footprint of quarks and gluons produced at high transverse momentum (p_{T}). The measurement of the energy of jets plays an important role for all jet-based measurements at the ATLAS experiment, and the uncertainty in the jet energy calibration often limits the precision of important physics results.

In ATLAS, the jet energy measurement [1–5] relies on corrections based on Monte Carlo (MC) simulations modelling the detector response and by assessing in situ how well the MC simulations describe data. The calibration of the average jet p_{T} is called the 'jet energy scale' (JES) and consists of several steps. The first correction based on MC simulations ensures that the reconstructed jet energy equals, on average, the energy of the corresponding jet formed by stable particles interacting with the ATLAS detector. Several effects are corrected including the non-compensating nature of the ATLAS calorimeter having a lower response to hadrons than to electrons or photons, energy deposits outside jets and energy losses in dead material before and in between the calorimeters. The jet response is also equalized as function of variables, like, e.g. the energy fraction in the hadronic calorimeter or the number of tracks, that are sensitive to jet fragmentation. In this procedure the average jet response is not changed, but the jet resolution is improved. In a final step of the jet calibration, the detector response to the jet in the MC simulation is compared to the one in the data by exploiting the p_{T}-balance in certain event topologies where the jet recoils against a well-measured object like a photon or a Z boson decaying into electron or muon pairs (Z/γ+jet).

The jets are first calibrated in the central region of the detector. The p_{T}-balance in dijet events with a central and a forward jet extends this calibration to more forward regions. At higher p_{T}, the uncertainties associated with this extrapolation tend to be sub-dominant such that the primary motivation to improve the precision of the jet energy calibration with independent methods is in the central region of the detector. In this paper, the focus is therefore on the most central pseudo-rapidity region $|\eta| < 0.8$.[1]

⋆ e-mail: atlas.publications@cern.ch

[1] ATLAS uses a right-handed coordinate system with its origin at the nominal interaction point (IP) in the centre of the detector and the z-axis along the beam pipe. The x-axis points from the IP to the centre of the LHC ring, and the y-axis points upwards. Polar coordinates (r, ϕ) are used in the transverse plane, ϕ being the azimuthal angle around the

Published online: 01 September 2025

In the standard jet calibration methods, the main systematic uncertainties are related to the knowledge of the p_{T}-balance in Z/γ+jet event topologies in data and MC simulation. Since jets are composed of collections of single particles, the single-particle response measurements can be used to derive the JES and the corresponding JES uncertainties. During the beginning and end of the LHC Run 1, ATLAS derived the data-to-MC jet response correction using calorimeter response measurements of single particles from pp collisions at $\sqrt{s} = 7$ and $\sqrt{s} = 8$ TeV [6,7] and relied on test-beam measurements for particles in the high-p_{T} regime. The data-to-MC response shift was compatible with the one derived from the p_{T}-balance based methods, but the resulting uncertainty was larger. Therefore, the single-particle-based uncertainty was only used for very high-p_{T} jets beyond the kinematic reach of the p_{T}-balance based methods. A similar method was also used for the determination of the τ-lepton energy scale for hadronic τ-lepton decays at a collision energy of 8 TeV [8].

In Run 1, the single-hadron response measurements, i.e., the ratio of the calorimeter energy to the momentum of an isolated track (E/p), were only performed in minimum bias collisions. The kinematic reach was limited to a track p_{T} of 20−30 GeV, since high-p_{T} tracks are preferentially found within jets and are not isolated. The higher p_{T} range was therefore covered with pre-data-taking test-beam measurements where a complete slice of the ATLAS detector was exposed to pion beams [9]. Differences between particle types were studied with MC simulations.

In Run 2, where the LHC collided protons on protons at a centre-of-mass energy of 13 TeV, sufficiently large data sets were available to exploit isolated single pions resulting from the hadronic decay of τ-leptons produced in W boson decays ($W \to \tau\nu$). The E/p response for isolated pions from τ-lepton decays was measured for $10 < p_{\mathrm{T}} < 300$ GeV with small uncertainties (below 1.5%) [10]. This much larger kinematic reach and the small associated uncertainty opened up a new level of precision for the JES.

This paper presents the JES and the corresponding uncertainty derived from single-particle response measurements and MC simulation studies. It is derived for anti-k_t-jets [11] with a nominal radius parameter $R_{\mathrm{jet}} = 0.4$, and clustered using the FastJet package [12,13]. Only the central pseudo-rapidity region $|\eta| < 0.8$ is used. The other calorimeter regions can be calibrated with the in situ dijet pseudo-rapidity intercalibration method where the forward jet is balanced by a central jet [1–5]. The single-particle response method also allows for the derivation of the JES calibration factors and the uncertainties for quark- and gluon-induced jets, and for different jet definitions such as for varying the chosen value of R_{jet} parameters.

The jets are formed from topological clusters of calorimeter cells [14] on the electromagnetic scale[2] (EMTopo) and are corrected with a MC-based calibration [1,4,15,16]. The JES derived from single-particle measurements is compared to that obtained from the in situ p_{T}-balance based methods, and subsequently, combined with it. Since the uncertainties of the two methods are largely independent and of somewhat similar amplitude the combination gives significant improvements. The combination for particle-flow (PFlow) jets [2], where the information from the tracking and calorimeter system is combined to achieve optimal performance, is only performed in a restricted jet p_{T} range.

The paper is structured as follows: Sect. 2 briefly describes the ATLAS detector and the MC simulation. The method to derive the JES from single-particle response measurements (deconvolution method) is described in Sect. 3. The input measurements and their systematic uncertainties are explained. The final results of the JES together with a detailed break-down of the uncertainties are presented in Sect. 4 for quark- and gluon-initiated jets separately. The results are compared to the ones obtained with the Z/γ+jets methods. Section 5 presents the combination of the JES obtained with the deconvolution method and with the Z/γ+jets method. The new uncertainties are compared to the ones previously available for physics analyses in Sect. 6.

In Sect. 7 the JES is obtained for jets with various radius parameters scanned from 0.2 to 1.0. Differences between inclusive jets produced by strongly interacting particles and jets from boosted top quarks with and without grooming soft jet constituents are studied. Finally, the conclusions are given in Sect. 8.

2 ATLAS detector and Monte Carlo simulation

The ATLAS experiment [17] at the LHC is a multipurpose particle detector with a forward–backward symmetric cylindrical geometry and a near 4π coverage in solid angle. It consists of an inner tracking detector surrounded by a thin superconducting solenoid providing a 2 T axial magnetic field, electromagnetic and hadronic calorimeters, and a muon spectrometer. The inner tracking detector covers the pseudo-rapidity range $|\eta| < 2.5$. It consists of silicon pixel, silicon microstrip, and transition radiation tracking detectors. Lead/liquid-argon (LAr) sampling calorimeters pro-

z-axis. The pseudorapidity is defined in terms of the polar angle θ as $\eta = -\ln\tan(\theta/2)$ and is equal to the rapidity $y = \frac{1}{2}\ln\left(\frac{E+p_z c}{E-p_z c}\right)$ in
Footnote 1 Continued
the relativistic limit. Angular distance is measured in units of $\Delta R \equiv \sqrt{(\Delta y)^2 + (\Delta\phi)^2}$.

[2] The electromagnetic scale is the calibration of the ATLAS calorimeter that ensures that the energy deposited by electromagnetic showers is correctly measured.

vide electromagnetic (EM) energy measurements with high granularity within the region $|\eta| < 3.2$. A steel/scintillator-tile hadronic calorimeter covers the central pseudo-rapidity range ($|\eta| < 1.7$). The endcap and forward regions are instrumented with LAr calorimeters for EM and hadronic energy measurements up to $|\eta| = 4.9$. The muon spectrometer surrounds the calorimeters and is based on three large superconducting air-core toroidal magnets with eight coils each. The field integral of the toroids ranges between 2.0 and 6.0 T m across most of the detector. The muon spectrometer includes a system of precision tracking chambers up to $|\eta| = 2.7$ and fast detectors for triggering up to $|\eta| = 2.4$. The luminosity is measured mainly by the LUCID–2 detector located close to the beam-pipe. A two-level trigger system is used to select events [18]. The first-level trigger is implemented in hardware and uses a subset of the detector information to accept events at a rate below 100 kHz. This is followed by a software-based trigger that reduces the accepted event rate to 1 kHz on average, depending on the data-taking conditions in the LHC Run 2.

A software suite [19] is used in data simulation, in the reconstruction and analysis of real and simulated data, in detector operations, and in the trigger and data acquisition systems of the experiment. The ATLAS detector is modelled with a detailed simulation [20] based on GEANT4 [21]. The hadronic shower simulations mainly consist of three kinematic regions: physics interactions of the nucleus for momenta of the incident particles around 1 GeV (pre-compound model), nucleon-nucleon cascades in the nucleus in the medium p_{T} region, and the modelling of the nuclear break-up for high p_{T}. The choice of the models as function of the kinematic regime is called the 'physics list' in the GEANT4 simulation. The ATLAS default simulation is based on the `FTFP_BERT_ATL` [22] physics list. In this physics list the *Bertini cascade model* [23] is used for hadrons with energy below 12 GeV, and the *Fritiof string model* [24,25] to model the nuclear break-up for hadrons with energy above 9 GeV. The probability of using each model changes smoothly across the region of overlap.

As alternative to the Bertini cascade model and the Fritiof model, the *quark gluon string model* (QGSP) [26] and the *binary cascade model* [27] are used for systematic studies. Other variations include a high-precision tracking of electromagnetic showers and very low energy neutrons, a different set of elastic pp cross-sections and a different treatment of diffractive processes. Further systematic uncertainties are estimated by using simulations with varied detector geometries. The material in the inner detector is increased in specific regions and overall by 5% and material is added between the electromagnetic and the hadronic calorimeters. Moreover, the detector geometry is distorted in the inner detector end plate, the cryostat and before and after the calorimeter presampler. These variations are constructed based on the degree of knowledge of the detector geometry based on measurements taken during construction and studies of interactions in the inner detector [28].

The nominal MC simulation of a sample of inclusive dijet events is the same as used in the calibration of jets in ATLAS [1–5]. It is produced using PYTHIA 8.235 [29] with the A14 set of tuned parameters [30]. PYTHIA uses a leading-order $2 \to 2$ matrix element interfaced with a parton distribution function (PDF) to model the hard process. The PDF used is NNPDF2.3LO [31]. Additional radiation is modelled in the leading-logarithm approximation using p_{T}-ordered parton showers. Multiple parton-parton interactions and underlying event are also simulated. Hadronisation is based on the Lund string model [32,33], and EVTGEN 1.6.0 [34] is used to decay heavy hadrons.

An alternative sample of inclusive dijet events is generated with SHERPA 2.2.11 [35] with the CT14nnlo PDF [36]. A leading-order $2 \to 2$ matrix element is interfaced with a parton shower using Catani–Seymour dipole factorisation [37]. The cluster based hadronisation module AHADIC++ [38] is used with re-tuned parameters that improve agreement with the LEP data of the fractions of different hadrons within hadronic jets [39]. The internal HADRONS++ module is used to decay heavy hadrons.

The JES of large-R_{jet} jets, where boosted top quarks and W bosons are merged in one large jet, is studied using a sample with new hypothetical heavy Z bosons (Z') that further decay into top quark pairs. This sample is simulated using PYTHIA 8.212 with the A14 tune and the leading-order NNPDF2.3LO PDFs. The cross-section of the hard-scattering process and the branching fractions were modified such that a fairly flat jet p_{T} spectrum is obtained between 250 GeV and 1.5 TeV for b-jets, c-jets, and light-flavour jets, with a falling tail of the p_{T} distribution populated to 3 TeV for each flavour.

Furthermore, simulated inclusive inelastic pp collisions were overlaid to model additional pile-up collisions in the same and neighbouring bunch crossings. These were generated with PYTHIA 8.186 [40] using the NNPDF2.3LO PDFs and the A3 set of tuned parameters [41].

3 Deconvolution method and input measurements

The jet energy calibration corrects the measured jet energy for several effects like calorimeter non-compensation, energy losses in the dead material or energy deposited outside the jet. In a first step it is derived from MC simulation comparing the reconstructed and the true jet energy.[3] In a second step, the

[3] The true jet energy is derived from the stable particles associated with the jet with a proper lifetime $c\tau > 10$ mm (excluding neutrinos and muons) impinging the ATLAS detector as given by the MC simulation before any detector simulation.

calorimeter response to jets in data and MC is evaluated, and the data-to-MC ratio is used as the jet energy response correction. In the deconvolution method [6,7], the jet response correction is determined by viewing the reconstructed jet as a superposition of energy depositions from the single particles constituting the jet. This method is based on MC simulation, but uses single-particle calorimeter response measurements for various particle types in data and MC to compute the data-to-MC jet response correction. A schematic overview of the method is shown in Fig. 1.

In the ATLAS MC simulation, the energy depositions produced in the ATLAS detector by each individual particle, called 'truth' particle in the following, can be identified. Therefore for each energy deposition in the calorimeter the kinematics and the particle type (electron, photons, pions, protons etc.) are known. The energy depositions of the particles associated to jets can be used to calculate data-to-MC jet response corrections using measurements of the calorimeter response to single particles in data and MC simulation. For each calorimeter cell associated to the reconstructed jet, the energy deposits of the truth particles are identified and corrected by the measured ratio between data and MC of the calorimeter response to an isolated particle of the corresponding particle type with the same kinematics.

The ratio of the total energy depositions within the jet after and before the correction gives the data-to-MC jet response correction (R_{Data}/R_{MC}). The mean of this jet response correction is used for jet calibration.

The data-to-MC jet energy correction uncertainty is calculated from the single-particle response uncertainties. Each uncertainty component in the single-particle response gives an independent uncertainty component for the JES. The numerical evaluation of the uncertainty in the JES is performed with MC pseudo-experiments. In each pseudo-experiment, the jet energy scale correction is calculated after randomly varying the MC single-particle energy response within the appropriate uncertainty range, as given by the measured single-particle data-to-MC ratio. Each particle is treated independently. The final JES uncertainty is then derived from the spread of the distribution of the jet energy scale over all pseudo-experiments.

The sequence of the randomly changed parameters are kept fixed within each pseudo-experiment such that the energy response correlations are properly taken into account. This method is chosen as different truth jets have different spectra of truth particle energies and types, and with this method the average corrections for all jets as a function of p_T can be obtained.

The measured data-to-MC single-particle energy shifts and the corresponding uncertainties depend on the particle type and the kinematic range. They are obtained from measurements of the single-particle response in data and MC simulation. The calorimeter response to single charged hadrons E/p is defined as the ratio of the average energy deposited by an isolated charged particle in the calorimeter (E) to the momentum of its inner detector track (p).

The E/p measurement for single pions with $10 < p_T < 300$ GeV is performed using W bosons decaying into τ-leptons where the τ-lepton decays into a pion. The W bosons are produced by the W+jets process or in $t\bar{t}$ events from pp collisions at 13 TeV using the full Run 2 data sets corresponding to an integrated luminosity of 139 fb^{-1}. A missing transverse momentum trigger is used. The τ-leptons are selected as isolated tracks which predominantly selects one-prong decays. The effect of the neutral pions that can be produced in τ-lepton decays is substracted on a statistical basis. More details can be found in Ref. [10]. The measurements of single charged hadrons for $p_T < 10$ GeV were performed following the methodology of Ref. [7] using a minimum bias data sample obtained in pp collisions at 13 TeV from a special dedicated low pile-up run where an average of two additional collisions are expected. Both of the measurements use data sets processed employing the same thresholds for pile-up noise suppression corresponding to Run 2 pile-up conditions. The measurement of the electron and photon energy scale and uncertainty is performed using a tag-and probe technique in a data set with Z bosons decaying into electron pairs [42,43]. It also uses the full Run 2 13 TeV data set corresponding to an integrated luminosity of 139 fb^{-1}.

For all hadron types the same data-to-MC corrections are used. To account for differences of the calorimeter response to hadrons of other types, additional systematic uncertainties are estimated from MC simulation or previous measurements. Jet fragmentation effects are addressed by comparing the results obtained with the PYTHIA MC event generator with the ones from SHERPA.

The kinematic ranges of the single-particle measurements and the uncertainty estimations are summarised in Table 1 and explained in more detail in the following.

Systematic uncertainties in the E/p **measurement in the** $W \to \tau\nu$ **sample**

The statistical uncertainty in the E/p measurements in the $W \to \tau\nu$ sample is treated as a systematic uncertainty in the JES. Possible variations of the background relative to the single-pion signal from τ-lepton decays, i.e. muons, electrons or jets with extreme fragmentation patterns, are estimated by varying selection criteria. The peak of the E/p distribution is determined using a fit to a Gaussian distribution and an empirically found Landau distribution to account for background events. The systematic uncertainties are estimated from the fit closure in a MC sample and by varying the shape of the background distribution using different MC generators. Moreover, the simulated response of the background from additional π^0 in τ-lepton decays is considered.

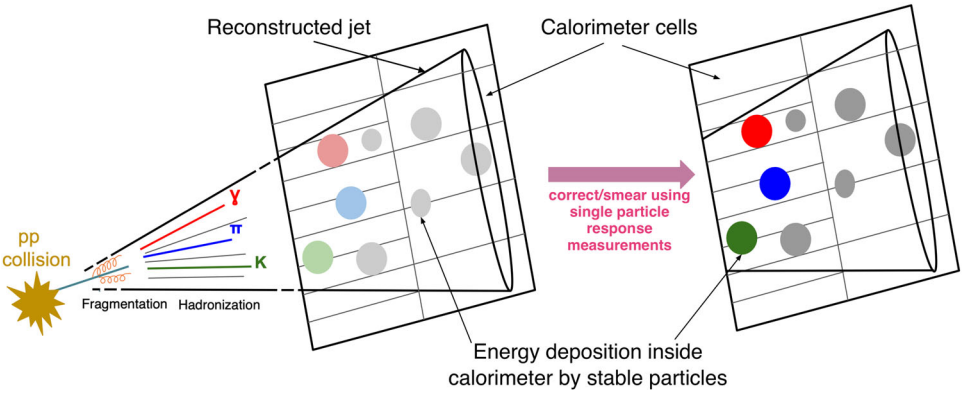

Fig. 1 Sketch of the particles associated with a jet and the corresponding energy depositions in the calorimeter. The colors represent the energy depositions of the various particle types. In the deconvolution method, the energy depositions are corrected and smeared to obtain the data-to-MC jet energy correction from calorimeter response measurements to single particles

Table 1 Overview of the input measurements and uncertainties used by the deconvolution method used for the calculation of the data-to-MC jet response correction

Particle	p_{T} [GeV]	Comment
Hadrons	$p_{\mathrm{T}} < 0.5$	5% uncertainty
	$0.5 < p_{\mathrm{T}} < 10$	Isolated tracks in minimum bias collisions
	$10 < p_{\mathrm{T}} < 300$	Pions from τ-lepton decays in $W \to \tau\nu$ sample
	$p_{\mathrm{T}} > 300$	MC out-of-range studies and using JES uncertainty constraint
e/γ	$5 < p_{\mathrm{T}} < 200$	Standard e/γ calibration from $Z \to e^+e^-$ and 0.5% uncertainty for effects in jets
	$p_{\mathrm{T}} > 200$	Extrapolation based on electron calibration
	$p_{\mathrm{T}} < 5$	Additional 1% uncertainty from $\pi^0 \to \gamma\gamma$ mass peak constraint

The energy deposition from pile-up events is subtracted on a statistical basis using the same technique as used for jets based on the event p_{T}-density (ρ) [44]. The non-closure of the pile-up correction and possible mis-modelling of pile-up effects is estimated by splitting the data sample into two samples with an average of low (20) and high (50) number of pile-up events.

Biases in the track momentum measurement are addressed by modifying the event selection such that the isolated track is matched to a muon allowing for a cross-calibration of the track p_{T} to the muon p_{T} that is well measured using Z bosons decaying into muon pairs [45]. The statistical uncertainty as well as the muon track calibration uncertainties are considered. Effects from the muon track resolution which depend on the underlying p_{T} spectrum are evaluated as well. Further details on the relative sizes of these components as a function of p_{T} can be found in Ref. [10]. A flat uncertainty of 0.15% is used that is also in line with the studies on the sagitta bias using J/Ψ and Z boson decays into muon pairs [46].

Systematic uncertainties in the E/p measurement in the minimum bias sample

The largest systematic uncertainty in the E/p measurement in the minimum bias sample is due to the cluster seeding probability, which gives the fraction of charged isolated hadrons that deposit energy in the calorimeter that is too low compared with the noise thresholds. The ratio of the cluster seeding probability in data and MC is taken as a systematic uncertainty. This uncertainty is about 30% up to about 1 GeV, 10% between 2 and 3 GeV and it is negligible at 10 GeV. Since the cluster seeding probability might be different for isolated single particles or particles within jets, the full effect is treated as an uncertainty and not as a jet response correction.

As a cross-check the energy fraction of truth particles depositing no energy in the calorimeter was also evaluated in the MC simulation. If the total amount of this energy fraction is taken as uncertainty, this method gives as expected a somewhat smaller uncertainty as for example it does not include effects from the noise thresholds of the topological clusters.

An additional 5% uncertainty is taken for charged hadrons below the measured range, i.e. $p_{\mathrm{T}} < 0.5$ GeV as estimated in Ref. [7]. Even with this large uncertainty the energy depositions of such low-p_{T} hadrons have a negligible effect, since they amount to only a tiny fraction of the jet energy. The statistical uncertainty in the E/p measurement is also considered. The same uncertainty in the track momentum measurements as in the $W \to \tau\nu$ E/p measurement is used. Effects from pile-up collisions are estimated by comparing the E/p measurement in events with one and two additional collisions. The influence of neutral particles close to the isolated track used in the E/p measurements is estimated and subtracted using a data set where the energy deposit in the electromagnetic calorimeter is compatible with a minimum

ionising particle [7]. This uncertainty is estimated to be 1% (3%) for $p > 2$ GeV ($p < 2$ GeV).

Systematic uncertainties in electrons and photons

The electron and photon calibration in ATLAS uses a tag-and-probe technique in an event sample with Z boson decays ($Z \to e^+e^-$) exploiting the constraint of the Z boson mass and cross-checked with J/Ψ and $Z \to ll\gamma$ decays at low transverse energy [42,43]. The electron and photon calorimeter response is measured in data and MC for $p_{\mathrm{T}} > 5$ GeV. Since the standard electron and photon calibration applies to isolated particles, an additional uncertainty of 0.5% is estimated for effects in a jet environment and to take possible differences between electrons and photons into account. For momenta beyond the reach of the $Z \to e^+e^-$ in situ calibration, the standard extrapolation estimate based on the detailed knowledge of how electrons are measured with the ATLAS detector is used [42,47]. For lower momenta ($p_{\mathrm{T}} < 5$ GeV), the invariant mass of neutral pions decaying into two photons is reconstructed using a minimum bias data sample. The same energy shift between data and MC at higher momentum is found, but to stay conservative an additional uncertainty of 1% is applied to low energy electromagnetic energy deposits.

Modelling of various hadron types

The most abundant particle types in jets are charged and neutral pions, but some other particle types contribute as well. The hadronic interactions of baryons and mesons such as $\pi^{\pm}$, p, $\bar{p}$, n, $\bar{n}$, $K^{\pm}$, K_L, K_S, Λ etc. with the detector can lead to slightly different calorimeter responses [7]. The effect is small for particles with $p_{\mathrm{T}} > 20$ GeV, but can be sizeable for very low p_{T}. The baseline calibration and uncertainty derived for charged pions from the $W \to \tau\nu$ sample or a mixture of charged hadrons dominated by pions in the minimum bias sample is applied to all hadron types, but additional uncertainties are estimated for specific hadron types based on MC simulations.

Baryons produce less neutral pions and therefore the measured energy in the calorimeter is lower than for a pion with the same momentum. These effects are well simulated [7,48,49]. Studies using Λ baryon decays in pp collisions at 8 TeV show that the response of protons is about 10% lower than the one for pions for momenta between 1 and 7 GeV [7]. The MC simulation describes this effect within statistical uncertainties. Because of isospin symmetry neutrons behave similar to protons in the calorimeter. This is also confirmed by simulation studies showing that protons and neutrons have the same energy deposit over the studied kinematic range of $0.7 < p < 100$ GeV [7]. Possible differences between the proton and neutron response can be indirectly tested by studying the charge exchange reaction ($\pi^- p \to \pi^0 n$ versus $\pi^+ n \to \pi^0 p$). The calorimeter response to π^+ is about 10% higher than the one to π^- at $p = 1$ GeV, while the response becomes the same for $p > 3$ GeV [7]. The charge dependence at low p_{T} is caused by the higher density of neutrons relative to protons in the absorber material of the ATLAS electromagnetic calorimeter. The simulation describes the data within statistical uncertainties. Since, however, no direct constraints are available for neutrons and the above studies are statistically limited a conservative uncertainty of 10% (5%) is assigned for neutrons with $p < 3$ GeV ($p > 3$ GeV) [7].

The slightly different showering of charged kaons compared with pions is well simulated [48] and no additional corrections or uncertainties are taken into account. The long-lived neutral kaon (K_L) lifetime is such that they are likely to reach the calorimeter before decaying and will therefore start their hadronic shower in the calorimeter but some of them will decay before entering the calorimeter.

If they decay before the calorimeter the impinging particles are different than for a stable particle produced in the collisions. The uncertainties in the effect of long-lived neutral kaons on the jet energy measurement is addressed by varying shower simulation models and detector geometries in the MC simulation. Simulations of single particles in the ATLAS detector are used, with varied assumptions, including different models of how particles interact with the detector and different detector geometries.

The largest deviation of the response ratio of long-lived kaons and pions relative to the default simulation is 3% and is obtained when exchanging the Fritiof model with the QGSP model. The variations of the detector geometry are negligible. The uncertainty is estimated conservatively to cover the full deviation. For the region $p_{\mathrm{T}} < 25$ GeV a flat uncertainty of 3% is assumed, while for $p_{\mathrm{T}} > 25$ GeV the uncertainty is parameterised as $0.05 - 0.015 \cdot \log(p_{\mathrm{T}}/\mathrm{GeV})$.

Short-lived kaons (K_S) decay 70% of the time into $K_S \to \pi^+\pi^-$ and 30% into $K_S \to \pi^0\pi^0$. Above 27 GeV, a K_S on average travels over 1.47 m and, therefore, enters the calorimeter before decaying. At high momentum, K_S behaves similarly to K_L (having a similar mass and the same charge), and both of the particles produce showers in the calorimeter. Therefore, the same uncertainties as those for K_L are applied to K_S above 27 GeV. Below 27 GeV, the K_S decay mode is simulated according to the branching ratio, and either the charged pion uncertainties with half of the kaon momentum ($p(\pi) = 0.5p(K_S)$) or the photon uncertainties with $p(\gamma) = 0.25p(K_S)$ are applied.

The uncertainties in the various particle types are all applied on top of the pion uncertainties from the E/p measurements.

Extrapolation of the single-particle response to very high p_{T}

For very high-p_{T} jets, the extrapolation of the single-particle response beyond the measured kinematic range is important.

Two different methods are used to estimate this uncertainty. The first method is based on variations of the hadronic shower simulations. The second method explores the knowledge of the JES response of the p_{T}-balance based in situ methods at 2 TeV to constrain the JES derived from E/p measurements at high p_{T} by scanning various assumed values of the out-of-range particle uncertainty.

In the first method the single-particle simulations as described in Sect. 2 are used. All variations are forced to agree at $p_{\mathrm{T}} = 175$ GeV, where there are precise measurements from the $W \to \tau\nu$ data. Then the variation is studied as function of p_{T} up to 2 TeV. In addition, the energy is varied by 3% in the hadronic barrel and by 8% in the hadronic endcap calorimeter based on differences seen in the E/p measurement using τ-lepton decays [10]. The biggest effect is seen for the modelling of the nuclear break up for high-p_{T} jets using the QGS model instead of the Fritiof model. It can give a variation of up to 2% at the highest p_{T}. A simple parameterisation with a log-linear model, $0.02\ \log(p_{\mathrm{T}}/175\ \mathrm{GeV})$, is used to cover the deviation.

The uncertainty in the E/p measurement is assumed to remain constant beyond the last single-particle response measurement point. The extrapolation uncertainty is added in quadrature to the uncertainty in the E/p measurement.

The second method studies the effect of scanning the assumed value of the out-of-range uncertainty from 1% to 10% for particles outside of the kinematic reach of the E/p measurements. Previously 10% was assumed [6,7]. If the out-of-range single-particle response is changed up or down, the derived jet response is correspondingly changed at high p_{T}. For such a strong variation the JES derived from the E/p measurements is not compatible with the JES derived from in situ p_{T}-balance methods. The JES together with its uncertainty derived from the p_{T}-balance in situ methods therefore provides a constraint on the single-particle out-of-range response uncertainty. The particle spectra in the jet have large fluctuations and therefore particles at fixed p_{T} are contained in jets with a large range in jet p_{T}. The fraction of deposited energy by particles in a fixed p_{T} range increases for increasing jet p_{T}. Therefore, the knowledge of the JES response and of the corresponding uncertainty at a given p_{T} can be used to extrapolate to higher p_{T}. An uncertainty of 2% on the single-particle out-of-range uncertainty is evaluated following this procedure, resulting in a JES response uncertainty of 0.7% (0.8%) for a jet at $p_{\mathrm{T}} = 2$ (4) TeV. This result is similar to the extrapolation uncertainty estimated from the variations in the simulation of the ATLAS detector.

In the final JES uncertainty the out-of-range uncertainty from the MC model variations (first method) is used. This is a reduction of a factor of four compared with the previously assumed out-of-range JES uncertainty [6,7]. It is achieved by testing the detector modelling with in situ single-particle measurements covering a wide kinematic range and is supported through cross-checks using precise high-p_{T} jet response measurements to constrain the high-p_{T} single-particle response outside the p_{T} range where it is measured.

4 Jet energy scale for quark- and gluon-induced jets and comparison to p_{T}-balance methods

Since the deconvolution method relies on the MC simulations to determine the JES using the single-particle response measurements, the JES can be studied separately for quark- and gluon-induced jets. The standard ATLAS definition for jet studies to define the jet flavour is used, i.e. the flavour of the parton with the highest energy associated to the jet determines the jet flavour. The parton-to-jet association uses helper particles with negligible energy, but pointing in the same direction as the partons. These so-called 'ghost-particles' are clustered together with the stable particles by the jet algorithm following the method of Ref. [11]. The notion of a 'quark-initiated' or 'gluon-initiated' jet is not well-defined beyond leading-order in QCD [50,51], but it captures well the differences in the jet fragmentation. On average quark-initiated jets are narrower and have fewer constituents with a harder particle spectrum than gluon-initiated jets with the same p_{T}.

Figure 2a, b show the response shifts separately for gluon- and quark-induced jets for the main three single-particle measurements individually and the resulting total correction.

The individual corrections are obtained by selecting either electrons and photons (e/γ) or hadrons in exclusive kinematic domains at low p_{T} (E/p in the minimum bias data sets) or at high p_{T} (E/p in the $W \to \tau\nu$ data sets). The total correction is obtained using all particles. The jet response in data is lower than the one in MC. Therefore the jet response shift $(\mathrm{R_{Data}}/\mathrm{R_{MC}} - 1)$ is negative for both of the types of jets. The total jet response correction is about -5% at low-p_{T} and -2% at high-p_{T} for quark-induced jets. The response correction for gluon-induced jets is slightly more negative than the one for quark-induced jets. Gluon-induced jet have a softer fragmentation, resulting in a higher fraction of the total jet energy contained in low-p_{T} particles. The lower overall response shift is caused by the low-p_{T} measurements in the minimum bias data set. The correction for electrons and photons induces a shift of -1% at low p_{T} that gets a bit reduced towards higher p_{T}, i.e. for $p_{\mathrm{T}} = 4000$ GeV it is -0.4%. The single-hadron response measurement predicts a response shift of -4% at low p_{T} and no shift at high p_{T}. The single-pion measurement from the τ-lepton decays predicts a response shift of -0.2% at low p_{T} increasing to -1.5% for $p_{\mathrm{T}} = 4000$ GeV.

The individual uncertainties of the JES derived from the single-particle response measurements are shown in Fig. 2c, d as a function of the jet p_{T}. The e/γ uncertainties con-

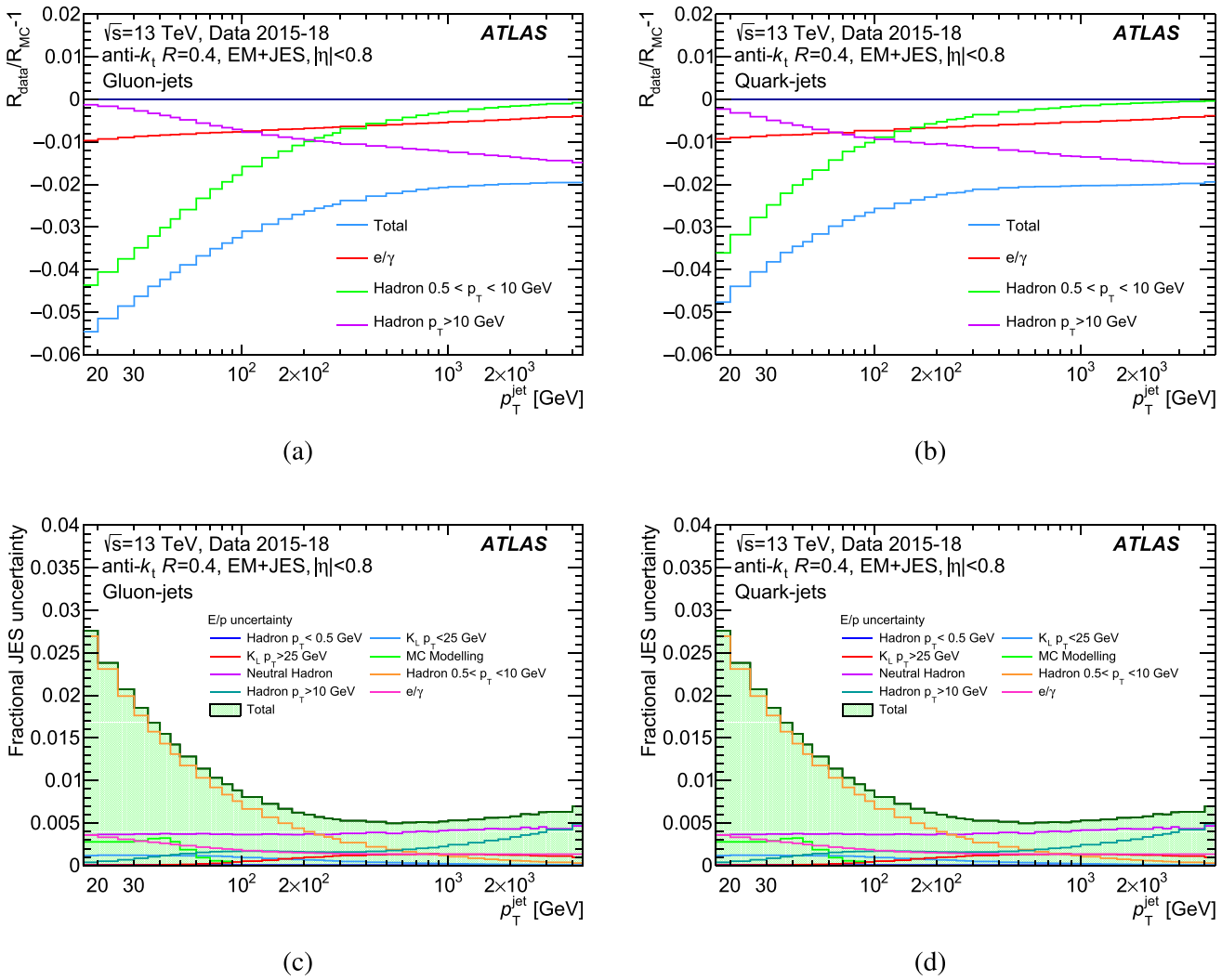

Fig. 2 Data-to-MC jet response shift for **a** gluon-induced and **b** quark-induced jets. The total correction and the individual shifts due to the e/γ correction, the single-hadron response measurement at low-p_{T} and the single-pion response at high-p_{T} are shown. The horizontal dark blue line indicates no correction. Fractional jet energy scale uncertainty derived from the E/p measurements as a function of the jet p_{T} for **c** gluon-induced and **d** quark-induced jets. The individual systematic uncertainties and the resulting total uncertainty are shown

tribute about 0.1% to 0.2% almost independent of p_{T}. The dominating uncertainty at low p_{T} is the uncertainty due to tracks that do not leave clusters in the calorimeter. This effect dominates the total uncertainty up to about $p_{\mathrm{T}} = 200$ GeV. In the range of $200 < p_{\mathrm{T}} < 2000$ GeV the largest single uncertainty is due to the calorimeter response to neutral hadrons. Beyond this p_{T} range the extrapolation uncertainty is largest. The uncertainties are slightly larger for gluon- than for quark-induced jets, since the uncertainty for low momentum particles have a higher impact on gluon-induced jets due to their softer fragmentation pattern.

The JES response and uncertainty as calculated from the single-particle measurement is shown in Fig. 3 as a function of the jet p_{T} together with the JES from the p_{T}-balance based in situ techniques. Here the jet response is calculated with the relative amount of quark- and gluon-induced jets (quark/gluon mixture) chosen to correspond to the expectation for jets in Z/γ+jets events. With this quark/gluon mixture a good agreement with the p_{T}-balance based method is obtained. However, any other quark/gluon composition would also give agreement within uncertainties.

The response shift between data and MC simulation of about -2% at high p_{T} obtained with two completely independent methods is very similar and well within the quoted uncertainties. The drop of the response ratio towards smaller p_{T} is also reproduced within uncertainties. The uncertainty from the single-particle response measurements is smaller than the one from the Z/γ+jet in situ methods for about $p_{\mathrm{T}} > 200$ GeV. The single-particle-based uncertainty smoothly and slowly increases towards the highest p_{T} values. At

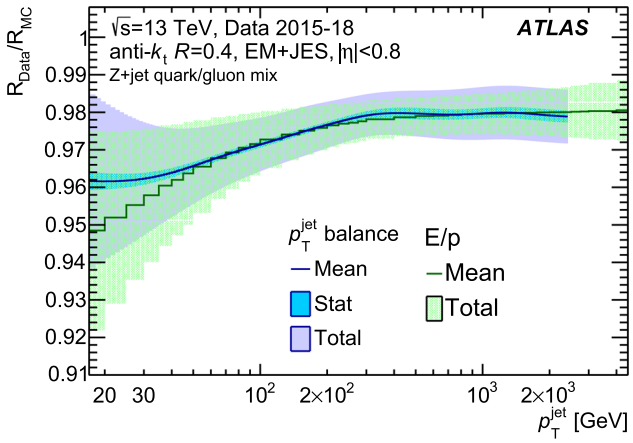

Fig. 3 Data-to-MC JES response ratio derived from the p_{T}-balance based in situ methods and the one from the single-particle response measurements (E/p) as a function of the jet p_{T}. The quark/gluon fractions as expected in the Z+jet process are used. The bands indicate the statistical and total uncertainties

2000 GeV the p_{T}-balance based JES uncertainty is 0.8% while the one from the single particles is 0.6%. The single-particle response measurement can be used for all jet p_{T}, i.e. also in the region where the p_{T}-balance based methods do not have kinematic reach.

5 Combination of single-particle response and p_{T}-balance methods

To achieve the highest precision determination of the jet energy scale corrections and uncertainties a combination of the results from single-particle response measurements and the p_{T}-balance based in situ techniques is performed. The combination is performed using a spline-based procedure, that has also been employed in e.g. Refs. [1,3,4,15,16,52] and references therein. Either linear or quadratic splines are used to interpolate between the various points of each in situ measurement and between the points of the E/p result. They are used to determine the contributions of each of these inputs in fine p_{T} bins.

An uncertainty propagation procedure, based on pseudo-experiments (propagating the full information of the input uncertainties with their correlations), allows to determine the covariance matrix of the various contributions in a given fine p_{T} bin. A weighted average of these contributions, based on a χ^2 minimisation, is then performed. The weights for the various in situ p_{T}-balance based and E/p inputs, computed taking into account the corresponding statistical and systematic uncertainties, should not be biased by the bin-size choices that were made for each of them. For this reason, the determination of the averaging weights is performed using in situ p_{T}-balance and E/p inputs that are first integrated into a common large binning, before performing the spline-based interpolation. The original in situ p_{T}-balance and E/p binning is employed afterwards, when performing the actual averaging using these weights.

While yielding a combined result that can be used for the jet energy calibration, it also allows for the evaluation of the level of agreement between the inputs. Each of the input uncertainties (i.e. nuisance parameters) is propagated through the combination procedure, by shifting the impacted inputs by one standard deviation of that uncertainty, re-doing the full averaging procedure and comparing the result with the nominal one. The fit quality is evaluated based on the χ^2/Ndof, where Ndof is the number of degrees of freedom. In case of some tensions between the inputs, identified through a $\chi^2/\mathrm{Ndof} > 1$ in a given bin, the propagated uncertainties are increased by a factor $\sqrt{\chi^2/\mathrm{Ndof}}$, following the recommendations of e.g. Ref. [53]. Finally, a Gaussian-kernel smoothing is applied coherently to the combination result and to its uncertainties.

The baseline result of this study, with the EMTopo jet collection, employs the precise E/p result down to p_{T} values of 17 GeV. The combination result, with the corresponding in situ p_{T}-balance and E/p inputs, the relative combination weights and the $\sqrt{\chi^2/\mathrm{Ndof}}$, as a function of the jet p_{T}, are shown in Fig. 4. In contrast to previous combinations [1,3,4,15,16,52], the results from the multi-jet balance (MJB) used to extend the p_{T}-range of the Z/γ+jet results are not used anymore, since the high-p_{T} region is now covered by the E/p measurements and which are more precise than the MJB method. The MJB results are in excellent agreement with the E/p measurements and while adding them does not give an uncertainty improvement, it would add a large number of small additional systematic uncertainty components. Thus the MJB is not included going forward.

The E/p result has a significant weight for the full p_{T} range and is the most significant contribution across the majority of the range where it is used. For instance, the weight of the E/p method increases with p_{T} from 10% at 40 GeV to 75% at 1 TeV. At very low p_{T} like 20 GeV the weight is 70%, thus helping to reduce the large uncertainty from the $Z+$jets modelling. The in situ p_{T}-balance based and the E/p inputs are also in good agreement over the full p_{T} range with a χ^2/Ndof around 0.5 in most of the p_{T}-range. At 100 GeV the χ^2/Ndof is around 1.

In Run 2 most ATLAS physics results are based on the PFlow jet reconstruction algorithm [2] where tracks and calorimeter-clusters are combined to improve the jet resolution and to mitigate pile-up effects. The PFlow algorithm benefits from the fact that charged hadrons at low p_{T} can be better measured with the tracking detector than with the calorimeter. Moreover, the tracks can be better assigned to the hard scattering vertex and therefore the rejection of pile-up contributions is easier. At high p_{T}, however, charged hadrons

can be better measured with the calorimeter and the contribution from tracks becomes minimal. The response of jets based on the PFlow algorithm therefore tends to the one from EMTopo jets towards high-p_{T} [4].

In the ATLAS PFlow algorithm a decision is made for each track whether the associated energy deposit in the calorimeter can be accurately identified such that it can be subtracted and the track measurement used [4]. This is dependent on the track p_{T} and the energy density around the shower in the calorimeter as in dense environments this identification becomes difficult. To correct for non-compensation effects, for the particles where the subtraction is not performed a fraction of the track energy is still included in the jet. Importantly, for particles where this subtraction is not performed, the shifted calorimeter contributions can be used to evaluate the shift in the jet energy scale of PFlow jets. Since PFlow jets also use tracks to reconstruct the jet energy, the jet response corrections take the reduced calorimeter energy fraction into account. For jets with $p_{\mathrm{T}} > 264$ GeV the fraction of the jet constituents where the subtraction is performed is below 5%, and thus the impact of track corrections is expected to be small. Therefore the single-particle technique can be applied to derive the jet energy response corrections and uncertainties. To avoid the region where this approximation might not be so accurate the combination of in situ p_{T}-balance techniques and single-particle response measurements is only performed above 300 GeV. The modelling of the charged-particle energy fraction in PFlow jets, i.e. the sum of the energy in tracks with respect to the jet p_{T}, was measured previously [2,16] and is well modelled. Therefore no additional uncertainty is added.

The combination result for PFlow jets, with the corresponding in situ p_{T}-balance based and E/p inputs, the relative combination weights and the $\sqrt{\chi^2/\mathrm{Ndof}}$, as a function of the jet p_{T}, are shown in Fig. 5. Here also, the E/p result has a relatively important weight on average, for the full p_{T} range where it is used. At 300 GeV it contributes about 20 %, at 1 TeV almost 80 and 100% for $p_{\mathrm{T}} > 1500$ GeV. The in situ p_{T}-balance based and E/p inputs are also in good agreement in the full p_{T} range where they overlap. The χ^2/Ndof is below 0.6 over the full p_{T} range where the combination is performed.

6 Comparison to previous results

The main part of the jet calibration is based on in situ techniques that assess the difference between data and Monte Carlo simulation of the calorimeter response to jets (JES from in situ calibration). The reduction in the jet calibration uncertainties for EMTopo jets is illustrated in Fig. 6a that compares the uncertainty obtained by the combination of the two in situ techniques discussed in this paper with the previous ones used in ATLAS measurements [4]. A significant improvement is seen for all values of jet p_{T}. The large improvement by a factor of 3 to 4 above roughly 2.5 TeV is mainly due to the larger kinematic range covered in the E/p measurements in the $W \to \tau\nu$ sample and the additional studies constraining the single-particle uncertainties beyond the measured range (see Sect. 3).

However, in addition to the in situ calibration JES uncertainties, there are also additional uncertainties to account for the dependence on the varying pile-up conditions (pile-up components) and on the flavour of the parton initiating the jet [1–5] (flavour components). Recently, significant progress has recently been made on the understanding of the calorimeter response to different jet flavours [54,55]. It was observed that the jet response difference between PYTHIA and HERWIG can be explained by the differences in the baryon fraction of the particles constituting the jet. SHERPA [56,57] using the cluster model [38,58] was in agreement with HERWIG but agreed with PYTHIA after a tuning of the baryon fraction to LEP data [39]. By calibrating the jet response in HERWIG [59,60] to the one in PYTHIA a large reduction of the flavour uncertainty was obtained. As a result the jet flavour uncertainty was reduced to a negligible level. Moreover, the flavour uncertainty was split into several components by comparing MC samples with different hadronisation models (string vs cluster model), different parton showers and different modelling of the hard scattering process (matrix element).

It is now interesting to see how both recent improvements compare to what is presently used in ATLAS physics analysis. Figure 6b shows the previous total JES uncertainty [4] and the one presented here for a quark/gluon mix in an inclusive dijet sample for PFlow jets. A significant improvement is seen for all jet p_{T}. Also shown are the additional uncertainties due to pile-up and to the jet flavour. The flavour uncertainty is very small (below 0.4% for $p_{\mathrm{T}} < 100$ GeV and negligibly small for $p_{\mathrm{T}} > 100$ GeV). The pile-up uncertainty is the largest uncertainty for jets below $p_{\mathrm{T}} < 100$ GeV. For higher p_{T} the uncertainties related to the in situ JES calibration are largest.

The total JES uncertainty amounts to about 4.0% at $p_{\mathrm{T}} = 20$ GeV, below 1% at $p_{\mathrm{T}} = 100$ GeV, 0.4% at $p_{\mathrm{T}} = 300$ GeV and 0.6% at $p_{\mathrm{T}} = 3$ TeV. The uncertainty at low p_{T} is dominated by the pile-up component but recently new pile-up subtraction techniques have been developed to significantly reduce these uncertainties [5]. The flavour uncertainties are significantly reduced by the updated treatment and the combination of in situ techniques with the newly derived corrections from single-particle measurements provide a significant reduction in this component above 400 GeV.

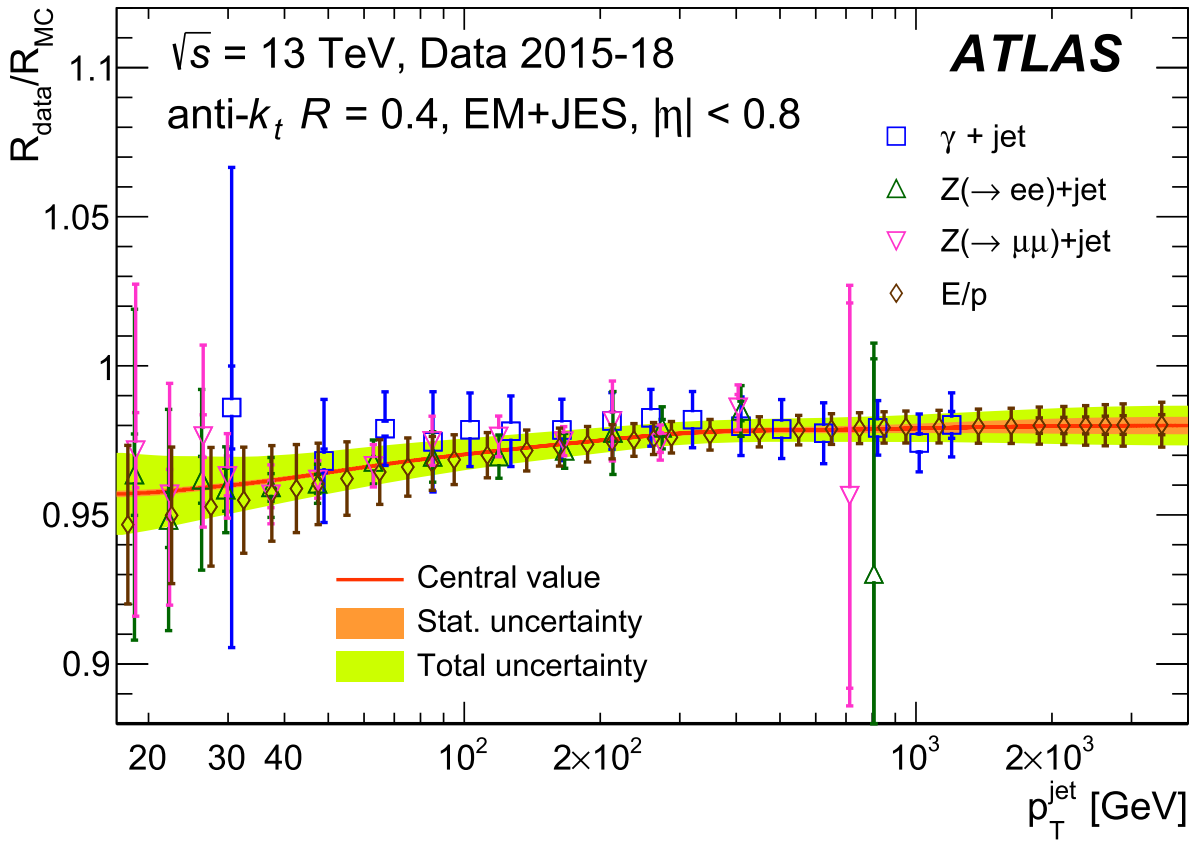

(a)

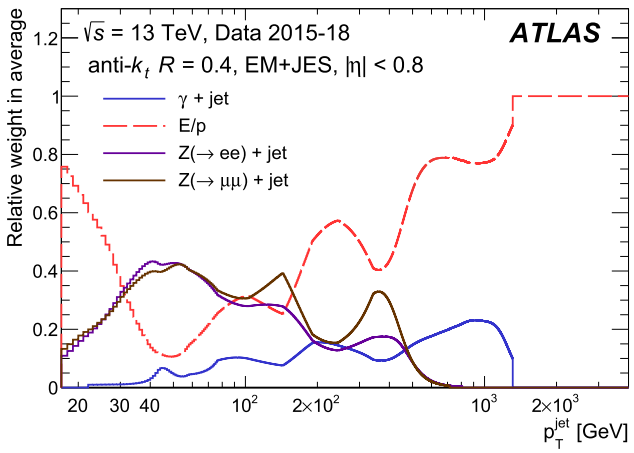

(b)

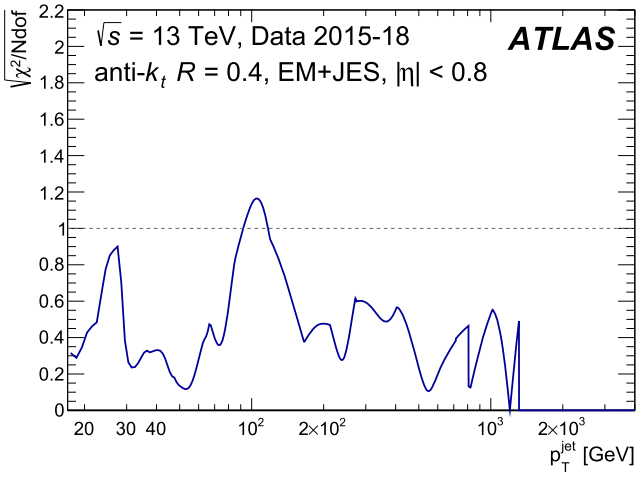

(c)

Fig. 4 Combination of the in situ E/p and p_{T}-balance (γ + jet and Z + jet) [5] results for the EMTopo jet collection. **a** Data-to-MC jet response ratio as a function of the jet p_{T}. The points indicate the various measurements with their statistical (inner bars) and systematic uncertainties added in quadrature (outer bars). The line indicates the nominal combination result, while bands indicate its statistical (inner bands) and total uncertainty (outer band) respectively. **b** The relative weights of the various input measurements used in the combination and **c** the $\sqrt{\chi^2/\mathrm{Ndof}}$ as a function of the jet p_{T}

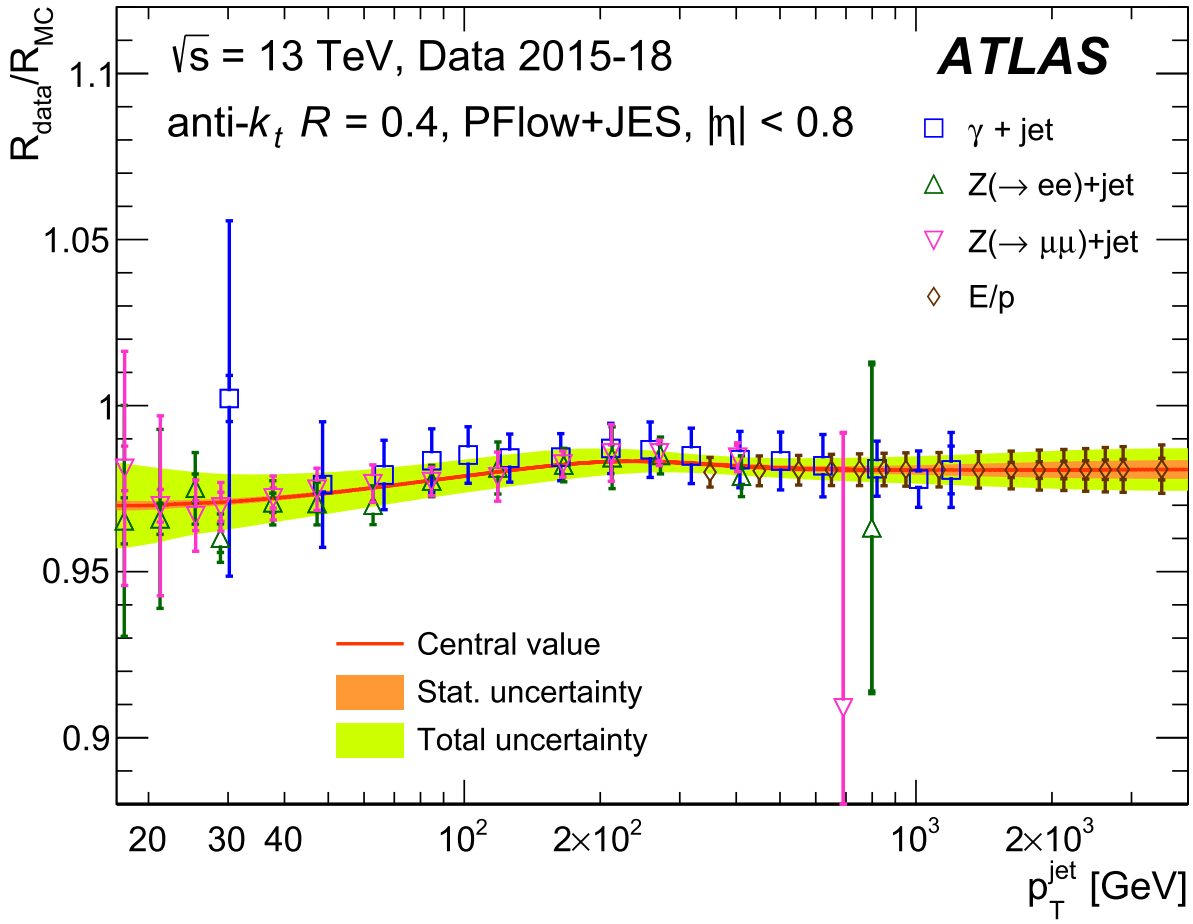

(a)

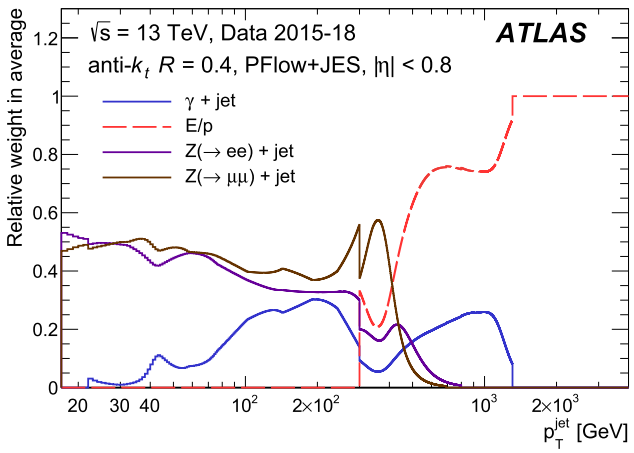

(b)

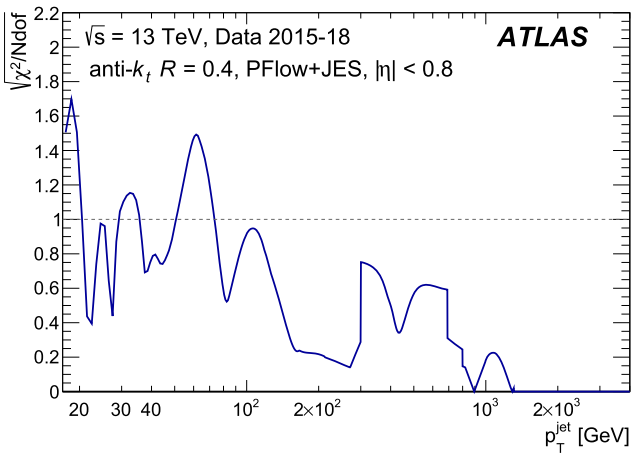

(c)

Fig. 5 Combination of the in situ E/p and p_{T}-balance (γ + jet and Z+jet) [5] results for the PFlow jet collection. **a** Data to MC jet response ratio as a function of the jet p_{T}. The points indicate the various measurements with their statistical (inner bars) and systematic uncertainties added in quadrature (outer bars). The line indicates the nominal combination result, while bands indicate its statistical (inner bands) and total uncertainty (outer band) respectively. **b** The relative weights of the various input measurements used in the combination and **c** the $\sqrt{\chi^2/\mathrm{Ndof}}$ as a function of the jet p_{T}

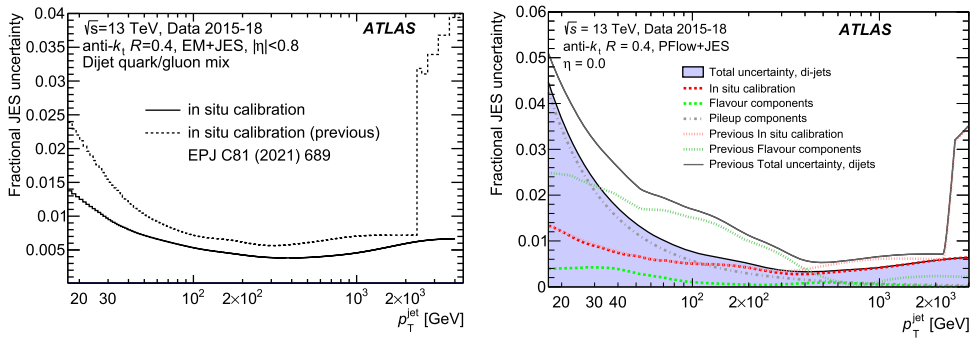

Fig. 6 **a** Fractional JES uncertainty in the data-to-MC response ratio from the in situ calibration using the new (solid) and the previously recommended JES uncertainty [4] (dashed) for EMTopo jets as a function of the jet p_{T}. **b** Total fractional JES for PFlow jets in the most central pseudo-rapidity region as a function of the jet p_{T}. In addition to the JES from the in situ calibration (red dashed line) the additional uncertainties due to the pile-up (grey dot-dashed line) and the jet flavour components added in quadrature (green dashed line) are shown. The blue area shows the quadrature sum of all the uncertainties. For comparison the uncertainties as previously recommended for physics analysis are also given: in situ calibration (red dotted line), flavour components (green dotted line) and total (solid grey line)

7 Jets with various radius parameters

The deconvolution method allows for the derivation of the data-to-MC response corrections for jets reconstructed with radius parameters of the anti-k_t jet algorithm different from the ATLAS default value ($R_{\mathrm{jet}} = 0.4$). In particular, studies of jet substructure for both small-R_{jet} and large-R_{jet} jets are interesting. In this section results are presented for R_{jet}-values ranging from 0.2 to 1.0. The JES can be studied with or without applying clustering algorithms to remove soft jet constituents (jet grooming).

Figure 7a shows the data-to-MC jet response correction together with their uncertainties for jets with radius parameters $R_{\mathrm{jet}} = 0.2$ and $R_{\mathrm{jet}} = 1.0$ divided by the one of $R_{\mathrm{jet}} = 0.4$ jets as a function of the jet p_{T}. Since the systematic uncertainties are correlated between the various R_{jet} values, the presentation of the results relative to the standard jets with $R_{\mathrm{jet}} = 0.4$ helps to better visualise the dependence of the jet response correction on the jet radius. The small radius jets have the smallest jet response correction and the largest radius jets the largest. At low p_{T} differences between the R_{jet} values up to about 3% are observed. At large p_{T} the differences are below 1%, but are still significant. For 1 TeV jets the response correction for $R_{\mathrm{jet}} = 1.0$ ($R_{\mathrm{jet}} = 0.2$) is 0.15% (0.06%) lower (higher) than the one for $R_{\mathrm{jet}} = 0.4$ jets. For jets with $p_{\mathrm{T}} > 2$ TeV the response shifts are within the systematic uncertainties.

Figure 7b shows the data-to-MC response correction as a function of the jet radius parameter for jets with $p_{\mathrm{T}} =$ 32 GeV and with 1008 GeV.[4] Here no ratio with respect to $R_{\mathrm{jet}} = 0.4$ is taken and the response correction can be seen together with the uncertainty for each jet radius. In this presentation the systematic uncertainties are strongly correlated across the R_{jet} bins. At $p_{\mathrm{T}} = 32$ GeV the $R_{\mathrm{jet}} = 0.2$ jets have a jet response shift of -3.5% while the largest jet with $R_{\mathrm{jet}} = 1.0$ has a response shift of -5.5%. For $p_{\mathrm{T}} = 1008$ GeV a smaller variation is observed with the jet radius. When taking the correlation between the jet radii into account, this variation is also significant.

Figure 8a, b show the response correction due to the various E/p measurements for the smallest ($R_{\mathrm{jet}} = 0.2$) and the largest ($R_{\mathrm{jet}} = 1$) R_{jet}-values as examples. The response shifts due to the measurements of electrons and photons and of high-p_{T} pions do not vary with the R_{jet}-value. However, the response shift due to the low-p_{T} single-hadron response measurement in minimum bias collisions has a strong variation with the R_{jet}-value that is responsible for the overall response shift. The response shift due to low-p_{T} particles changes from -2% to -5% for $p_{\mathrm{T}} = 30$ GeV. Since the response shift is driven by low-p_{T} particles measured in minimum bias events, the overall response correction does not depend on the R_{jet}-value at high-p_{T}. This indicates that the response difference between small-R_{jet} and large-R_{jet} jets, for quark- and gluon-induced jets, is mainly driven by low-p_{T} particles. This is in-line with ATLAS jet substructure measurements showing that the energy density is highest close to the jet axis and that only a relatively small energy fraction is located in the outer parts [61,62]. Therefore, when enlarging the jet radius the energy fraction in the low-p_{T} particles is increased thus leading to an increase of the overall uncertainty.

[4] A low-p_{T} and a high-p_{T} value is displayed as example. The quoted p_{T} values correspond to the beginning of the chosen p_{T} bin which is more relevant than the bin centre since in most physics processes the p_{T} distribution falls steeply.

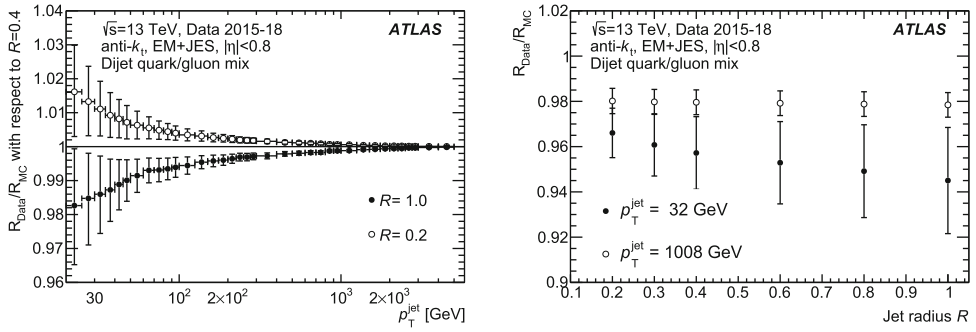

Fig. 7 **a** Data-to-MC JES response ratio derived from the single-particle response measurements for jets with $R_{\text{jet}} = 0.2$ and $R_{\text{jet}} = 1.0$ normalized to the one of jets with $R_{\text{jet}} = 0.4$ as a function of the jet p_{T}. The horizontal line at unity is drawn for better visibility. **b** Data-to-MC JES response ratio for jets with $p_{\text{T}} = 32$ GeV and $p_{\text{T}} = 1008$ GeV as a function of the jet radius. The error bars represent the quadrature sum of all the individual uncertainties. The flavour composition as in the inclusive dijet MC simulation is used

Figure 8c, d show the uncertainty for the two R_{jet} values discussed above. The uncertainty due to the E/p measurement in minimum bias events remains dominant, but its magnitude is smallest for small-R_{jet} values and largest for large-R_{jet} values. At $p_{\text{T}} = 30$ GeV it is about 1% for $R_{\text{jet}} = 0.2$ jets but is 3% for $R_{\text{jet}} = 1.0$ jets. At the highest p_{T} the variation is much less. The other uncertainties do not dependent on the R_{jet}-values.

These results are obtained for the standard jets formed by strongly interacting particles in dijet events. Large-R_{jet} jets are used to identify the decay products from boosted particles such as W/Z bosons or top quarks produced at large p_{T}. To reduce the increased sensitivity of large-R_{jet} jets to soft radiation, particles produced by the underlying event collisions or in pile-up pp interactions, grooming algorithms are applied that remove soft jet constituents based on a clustering algorithm running on the jet constituents. For an overview on this topic see Refs. [63,64].

In ATLAS the best performance of boosted particle reconstruction [65] is obtained for jets with $R_{\text{jet}} = 1.0$ that are used together with the soft drop clustering algorithm [66] with the radial distance parameter set to $\beta = 1.0$ and the soft-drop threshold set to $z = 0.1$.

Without further requirements on substructure variables to increase the fraction of jets with a two- or three-prong structure, the data-to-MC jet response correction is not changed for an inclusive jet sample. In an event sample with boosted top quarks produced by Z' boson decays to top quark pairs (see Sect. 2), the data-to-MC jet response correction with and without jet grooming is almost the same. For $p_{\text{T}} > 200$ GeV they agree within 0.1%. While grooming with the soft drop algorithm does not significantly modify the data-to-MC jet response correction, the origin of the jet does have an impact. For $p_{\text{T}} > 200$ GeV the response in the dijet sample is about 0.2% higher than in the Z' sample independent of p_{T}.

In summary, these studies show that differences of internal jet structure between inclusive jets and jets from boosted top-quark decays also lead to differences in the jet response correction, while the application of the soft-drop grooming algorithm with $\beta = 1.0$ and $z = 0.1$ has a negligible impact on the response of both the types of jets.

8 Conclusion

The jet energy scale correction together with the corresponding uncertainties has been derived from measurements of the calorimeter response to single particles of the ATLAS detector operating at the LHC. In particular, the measurements of isolated pions produced in τ-lepton decays have significantly increased the kinematic range where the calorimeter response to single pions has been measured in situ. As a result the jet energy scale correction uncertainty is significantly improved, reaching 2.5% at $p_{\text{T}} = 20$ GeV, 0.5% at $p_{\text{T}} = 300$ GeV and 0.7% at $p_{\text{T}} = 4$ TeV.

The results obtained from the single-particle measurements and the p_{T}-balance based method are in excellent agreement with the single-particle-based method having an improved accuracy. Since the uncertainties of the two measurements are uncorrelated, the combination of the two methods significantly improves the jet energy scale measurement with respect to earlier estimates. While low-p_{T} jets are still dominated by uncertainties related to pile-up, at $p_{\text{T}} = 300$ GeV and for PFlow jets the final JES uncertainty amounts to 0.3% and increases to 0.6% at $p_{\text{T}} = 3$ TeV.

Furthermore, the single-particle response method allows for the determination of the data-to-MC jet response correction for any jet collection definition, such as for variations of the jet radius parameter. Differences between jets of different radii are significant. While inclusive jets and jets

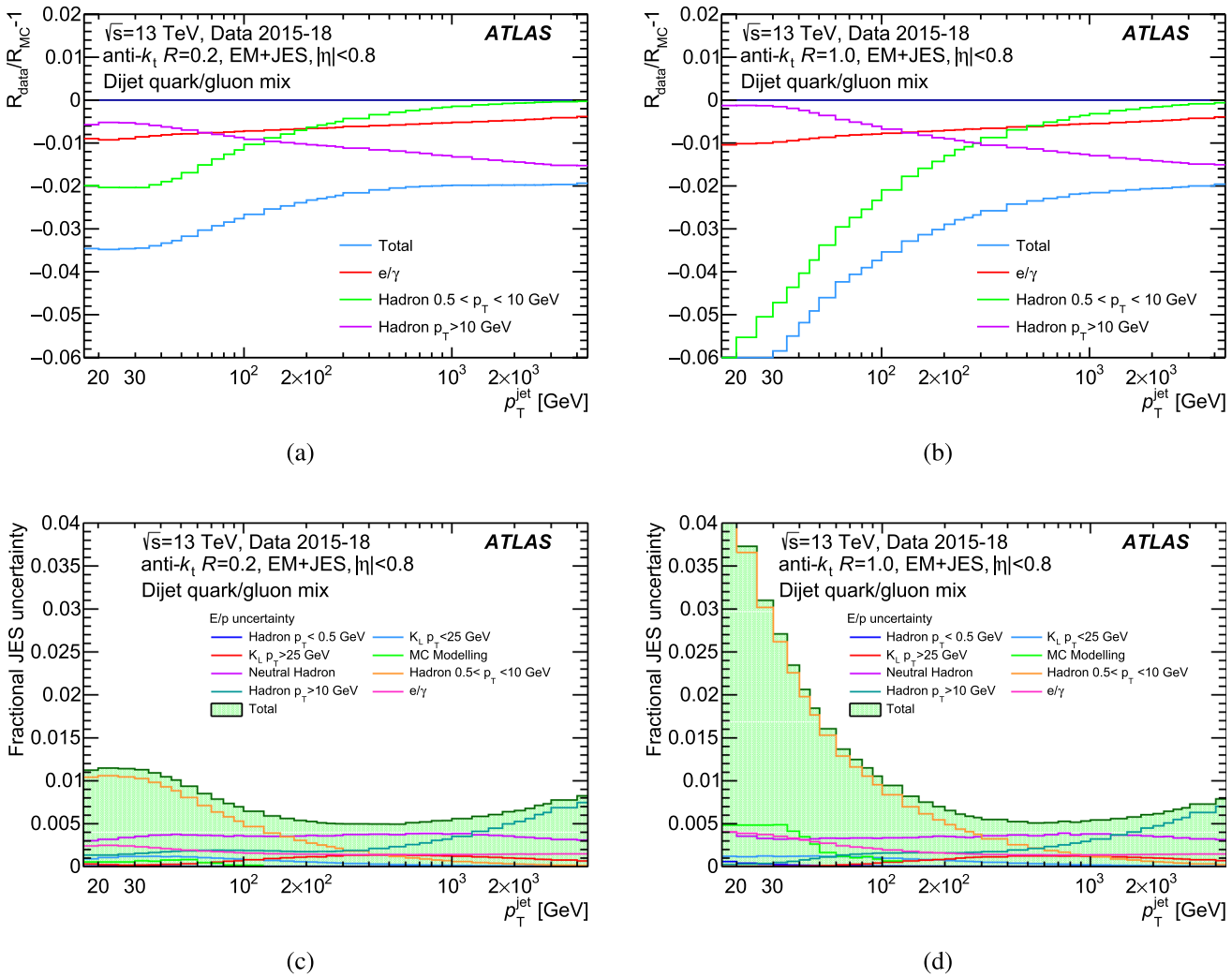

Fig. 8 Data-to-MC jet response correction derived from the E/p measurements as a function of the jet p_T with **a** $R_{jet} = 0.2$ and **b** $R_{jet} = 1.0$. Shown are the total correction together with the individual shifts due to the e/γ correction, the single-hadron response measurement at low-p_T and the single-pion response from τ-lepton decays at high-p_T. The horizontal black line indicates no correction. Fractional JES uncertainty derived from the E/p measurements as a function of the jet p_T for jets with **c** $R_{jet} = 0.2$ and with **d** $R_{jet} = 1.0$. The uncertainties are merged in classes for better visibility. The flavour composition as in the inclusive dijet MC simulation is used

from boosted top-quark decays have a jet response correction within 0.2% for $p_T > 200$ GeV, the application of the soft-drop grooming algorithm with $\beta = 1.0$ and $z = 0.1$ has a negligible impact on the response of both types of jets.

This analysis demonstrates a fundamental understanding of the jet energy measurement and a good description of the physics processes in the calorimeter by the MC simulation. The data-to-MC jet response shift as measured with the in situ p_T-balance based methods observed since the beginning of the data taking at the LHC can be shown to be due to the deficiencies of the MC simulation to describe the response of the ATLAS calorimeter to single particles. The jet response shift is primarily driven by the single hadron response modelling, but also has significant contributions from the modelling of electromagnetic processes.

The improvements in the jet energy calibration presented in this paper pave the way for precision jet measurements with the ATLAS detector.

Acknowledgements We thank CERN for the very successful operation of the LHC and its injectors, as well as the support staff at CERN and at our institutions worldwide without whom ATLAS could not be operated efficiently. The crucial computing support from all WLCG partners is acknowledged gratefully, in particular from CERN, the ATLAS Tier-1 facilities at TRIUMF/SFU (Canada), NDGF (Denmark, Norway, Sweden), CC-IN2P3 (France), KIT/GridKA (Germany), INFN-CNAF (Italy), NL-T1 (Netherlands), PIC (Spain), RAL (UK) and BNL (USA), the Tier-2 facilities worldwide and large non-WLCG resource providers. Major contributors of computing resources are listed in Ref. [67]. We

gratefully acknowledge the support of ANPCyT, Argentina; YerPhI, Armenia; ARC, Australia; BMWFW and FWF, Austria; ANAS, Azerbaijan; CNPq and FAPESP, Brazil; NSERC, NRC and CFI, Canada; CERN; ANID, Chile; CAS, MOST and NSFC, China; Minciencias, Colombia; MEYS CR, Czech Republic; DNRF and DNSRC, Denmark; IN2P3-CNRS and CEA-DRF/IRFU, France; SRNSFG, Georgia; BMBF, HGF and MPG, Germany; GSRI, Greece; RGC and Hong Kong SAR, China; ISF and Benoziyo Center, Israel; INFN, Italy; MEXT and JSPS, Japan; CNRST, Morocco; NWO, Netherlands; RCN, Norway; MNiSW, Poland; FCT, Portugal; MNE/IFA, Romania; MSTDI, Serbia; MSSR, Slovakia; ARIS and MVZI, Slovenia; DSI/NRF, South Africa; MICIU/AEI, Spain; SRC and Wallenberg Foundation, Sweden; SERI, SNSF and Cantons of Bern and Geneva, Switzerland; NSTC, Taipei; TENMAK, Türkiye; STFC/UKRI, United Kingdom; DOE and NSF, United States of America. Individual groups and members have received support from BCKDF, CANARIE, CRC and DRAC, Canada; CERN-CZ, FORTE and PRIMUS, Czech Republic; COST, ERC, ERDF, Horizon 2020, ICSC-NextGenerationEU and Marie Skłodowska-Curie Actions, European Union; Investissements d'Avenir Labex, Investissements d'Avenir Idex and ANR, France; DFG and AvH Foundation, Germany; Herakleitos, Thales and Aristeia programmes co-financed by EU-ESF and the Greek NSRF, Greece; BSF-NSF and MINERVA, Israel; NCN and NAWA, Poland; La Caixa Banking Foundation, CERCA Programme Generalitat de Catalunya and PROMETEO and GenT Programmes Generalitat Valenciana, Spain; Göran Gustafssons Stiftelse, Sweden; The Royal Society and Leverhulme Trust, United Kingdom. In addition, individual members wish to acknowledge support from Armenia: Yerevan Physics Institute (FAPERJ); CERN: European Organization for Nuclear Research (CERN PJAS); Chile: Agencia Nacional de Investigación y Desarrollo (FONDECYT 1230812, FONDECYT 1230987, FONDECYT 1240864); China: Chinese Ministry of Science and Technology (MOST-2023YFA1605700, MOST-2023YFA1609300), National Natural Science Foundation of China (NSFC - 12175119, NSFC 12275265, NSFC-12075060); Czech Republic: Czech Science Foundation (GACR - 24-11373 S), Ministry of Education Youth and Sports (FORTE CZ.02.01.01/00/22_008/0004632), PRIMUS Research Programme (PRIMUS/21/SCI/017); EU: H2020 European Research Council (ERC - 101002463); European Union: European Research Council (ERC - 948254, ERC 101089007), Horizon 2020 Framework Programme (MUCCA - CHIST-ERA-19-XAI-00), European Union, Future Artificial Intelligence Research (FAIR-NextGenerationEU PE00000013), Italian Center for High Performance Computing, Big Data and Quantum Computing (ICSC, NextGenerationEU); France: Agence Nationale de la Recherche (ANR-20-CE31-0013, ANR-21-CE31-0013, ANR-21-CE31-0022, ANR-22-EDIR-0002), Investissements d'Avenir Labex (ANR-11-LABX-0012); Germany: Baden-Württemberg Stiftung (BW Stiftung-Postdoc Eliteprogramme), Deutsche Forschungsgemeinschaft (DFG - 469666862, DFG - CR 312/5-2); Italy: Istituto Nazionale di Fisica Nucleare (ICSC, NextGenerationEU), Ministero dell'Università e della Ricerca (PRIN - 20223N7F8K - PNRR M4.C2.1.1); Japan: Japan Society for the Promotion of Science (JSPS KAKENHI JP22H01227, JSPS KAKENHI JP22H04944, JSPS KAKENHI JP22KK0227, JSPS KAKENHI JP23KK0245); Netherlands: Netherlands Organisation for Scientific Research (NWO Veni 2020 - VI.Veni.202.179); Norway: Research Council of Norway (RCN-314472); Poland: Ministry of Science and Higher Education (IDUB AGH, POB8, D4 no 9722), Polish National Agency for Academic Exchange (PPN/PPO/2020/1/00002/U/00001), Polish National Science Centre (NCN 2021/42/E/ST2/00350, NCN OPUS nr 2022/47/B/ST2/03059, NCN UMO-2019/34/E/ST2/00393, NCN & H2020 MSCA 945339, UMO-2020/37/B/ST2/01043, UMO-2021/40/C/ST2/00187, UMO-2022/47/O/ST2/00148, UMO-2023/49/B/ST2/04085, UMO-2023/51/B/ST2/00920); Slovenia: Slovenian Research Agency (ARIS grant J1-3010); Spain: Generalitat Valenciana (Artemisa, FEDER, IDIFEDER/2018/048), Ministry of Science and Innovation (MCIN & NextGenEU PCI2022-135018-2, MICIN & FEDER PID2021-125273NB, RYC2019-028510-I, RYC2020-030254-I, RYC2021-031273-I, RYC2022-038164-I), PROMETEO and GenT Programmes Generalitat Valenciana (CIDEGENT/2019/027); Sweden: Carl Trygger Foundation (Carl Trygger Foundation CTS 22:2312), Swedish Research Council (Swedish Research Council 2023-04654, VR 2018-00482, VR 2021-03651, VR 2022-03845, VR 2022-04683, VR 2023-03403), Knut and Alice Wallenberg Foundation (KAW 2018.0157, KAW 2018.0458, KAW 2019.0447, KAW 2022.0358); Switzerland: Swiss National Science Foundation (SNSF - PCEFP2_194658); United Kingdom: Leverhulme Trust (Leverhulme Trust RPG-2020-004), Royal Society (NIF-R1-231091); United States of America: U.S. Department of Energy (ECA DE-AC02-76SF00515), Neubauer Family Foundation.

Data Availability Statement This manuscript has no associated data. [Authors' comment: All ATLAS scientific output is published in journals, and preliminary results are made available in Conference Notes. All are openly available, without restriction on use by external parties beyond copyright law and the standard conditions agreed by CERN. Data associated with journal publications are also made available: tables and data from plots (e.g. cross section values, likelihood profiles, selection efficiencies, cross section limits, ...) are stored in appropriate repositories such as HEPDATA (http://hepdata.cedar.ac.uk/). ATLAS also strives to make additional material related to the paper available that allows a reinterpretation of the data in the context of new theoretical models. For example, an extended encapsulation of the analysis is often provided for measurements in the framework of RIVET (http://rivet.hepforge.org/).].

Code Availability Statement This manuscript has no associated code/software. [Authors' comment: ATLAS collaboration software is open source, and all code necessary to recreate an analysis is publicly available. The Athena (http://gitlab.cern.ch/atlas/athena) software repository provides all code needed for calibration and uncertainty application, with configuration files that are also publicly available via Docker containers and cvmfs. The specific code and configurations written in support of this analysis are not public; however, these are internally preserved.].

Funded by SCOAP[3].

References

1. ATLAS Collaboration, Determination of jet calibration and energy resolution in proton-proton collisions at $\sqrt{s}$ = 8 TeV using the ATLAS detector. Eur. Phys. J. C **80**, 1104 (2020). https://doi.org/10.1140/epjc/s10052-020-08477-8. arXiv:1910.04482 [hep-ex]
2. ATLAS Collaboration, Jet reconstruction and performance using particle flow with the ATLAS detector. Eur. Phys. J. C **77**, 466 (2017). https://doi.org/10.1140/epjc/s10052-017-5031-2. arXiv:1703.10485 [hep-ex]

3. ATLAS Collaboration, Jet energy scale measurements and their systematic uncertainties in proton-proton collisions at $\sqrt{s}$ = 13 TeV with the ATLAS detector. Phys. Rev. D **96**, 072002 (2017). https://doi.org/10.1103/PhysRevD.96.072002. arXiv:1703.09665 [hep-ex]
4. ATLAS Collaboration, Jet energy scale and resolution measured in proton–proton collisions at $\sqrt{s}$ = 13 TeV with the ATLAS detector. Eur. Phys. J. C **81**, 689 (2021). https://doi.org/10.1140/epjc/s10052-021-09402-3. arXiv:2007.02645 [hep-ex]
5. ATLAS Collaboration, New techniques for jet calibration with the ATLAS detector. Eur. Phys. J. C **83**, 761 (2023). https://doi.org/10.1140/epjc/s10052-023-11837-9. arXiv:2303.17312 [hep-ex]
6. ATLAS Collaboration, Single hadron response measurement and calorimeter jet energy scale uncertainty with the ATLAS detector at the LHC. Eur. Phys. J. C **73**, 2305 (2013).https://doi.org/10.1140/epjc/s10052-013-2305-1. arXiv:1203.1302 [hep-ex]
7. ATLAS Collaboration, A measurement of the calorimeter response to single hadrons and determination of the jet energy scale uncertainty using LHC Run-1 pp-collision data with the ATLAS detector. Eur. Phys. J. C **77**, 26 (2017).https://doi.org/10.1140/epjc/s10052-016-4580-0. arXiv:1607.08842 [hep-ex]
8. ATLAS Collaboration, Identification and energy calibration of hadronically decaying tau leptons with the ATLAS experiment in $P P$ collisions at $\sqrt{s}$ = 8 TeV. Eur. Phys. J. C **75**, 303 (2015). https://doi.org/10.1140/epjc/s10052-015-3500-z. arXiv:1412.7086 [hep-ex]
9. E. Abat et al., Study of energy response and resolution of the ATLAS barrel calorimeter to hadrons of energies from 20 to 350 GeV. Nucl. Instrum. Methods A **621**, 134 (2010). https://doi.org/10.1016/j.nima.2010.04.054
10. ATLAS Collaboration, Measurement of the energy response of the ATLAS calorimeter to charged pions from $W^{\pm} \to \tau^{\pm}(\to \pi^{\pm}\nu_{\tau})\nu_{\tau}$ events in Run 2 data. Eur. Phys. J. C **82**, 223 (2022).https://doi.org/10.1140/epjc/s10052-022-10117-2. arXiv:2108.09043 [hep-ex]
11. M. Cacciari, G.P. Salam, G. Soyez, The anti-k_t jet clustering algorithm. JHEP **04**, 063 (2008). https://doi.org/10.1088/1126-6708/2008/04/063. arXiv:0802.1189 [hep-ph]
12. M. Cacciari, G.P. Salam, G. Soyez, FastJet user manual. Eur. Phys. J. C **72**, 1896 (2012). https://doi.org/10.1140/epjc/s10052-012-1896-2. arXiv:1111.6097 [hep-ph]
13. M. Cacciari, G.P. Salam, Dispelling the N^3 myth for the k_t jet-finder. Phys. Lett. B **641**, 57 (2006). https://doi.org/10.1016/j.physletb.2006.08.037. arXiv:hep-ph/0512210
14. ATLAS Collaboration, Topological cell clustering in the ATLAS calorimeters and its performance in LHC Run 1. Eur. Phys. J. C **77**, 490, (2017).https://doi.org/10.1140/epjc/s10052-017-5004-5. arXiv:1603.02934 [hep-ex]
15. ATLAS Collaboration, Jet energy measurement and its systematic uncertainty in proton-proton collisions at $\sqrt{s}$ = 7 TeV with the ATLAS detector. Eur. Phys. J. C **75**, 17 (2015).https://doi.org/10.1140/epjc/s10052-014-3190-y. arXiv:1406.0076 [hep-ex]
16. ATLAS Collaboration, Jet energy measurement with the ATLAS detector in proton-proton collisions at $\sqrt{s}$ = 7 TeV. Eur. Phys. J. C **73**, 2304 (2013). https://doi.org/10.1140/epjc/s10052-013-2304-2. arXiv:1112.6426 [hep-ex]
17. ATLAS Collaboration, The ATLAS Experiment at the CERN large hadron collider. JINST **3**, S08003 (2008). https://doi.org/10.1088/1748-0221/3/08/S08003
18. ATLAS Collaboration, Performance of the ATLAS trigger system in 2015. Eur. Phys. J. C **77**, 317 (2017). https://doi.org/10.1140/epjc/s10052-017-4852-3. arXiv:1611.09661 [hep-ex]
19. ATLAS Collaboration, Software and computing for Run 3 of the ATLAS experiment at the LHC. (2024). https://doi.org/10.1140/epjc/s10052-010-1429-9. arXiv:2404.06335 [hep-ex]
20. ATLAS Collaboration, The ATLAS simulation infrastructure. Eur. Phys. J. C **70**, 823 (2010). https://doi.org/10.1140/epjc/s10052-010-1429-9. arXiv:1005.4568 [physics.ins-det]
21. S. Agostinelli et al., Geant4 – a simulation toolkit. Nucl. Instrum. Methods A **506**, 250 (2003). https://doi.org/10.1016/S0168-9002(03)01368-8
22. A. Ribon et al., Status of GEANT4 hadronic physics for the simulation of LHC experiments at the start of LHC physics program. CERN-LCGAPP 2 (2010). https://doi.org/10.1016/0029-554X(68)90054-2
23. M.P. Guthrie, R.G. Alsmiller, H.W. Bertini, Calculation of the capture of negative pions in light elements and comparison with experiments pertaining to cancer radiotherapy. Nucl. Instrum. Methods **66**, 29 (1968). https://doi.org/10.1016/0550-3213(87)90257-4
24. B. Andersson, G. Gustafson, B. Nilsson-Almqvist, A model for low-pT hadronic reactions with generalizations to hadron-nucleus and nucleus-nucleus collisions. Nucl. Phys. B **281**, 289 (1987). https://doi.org/10.1016/0550-3213(87)90257-4. (**issn: 0550-3213**)
25. B. Nilsson-Almqvist, E. Stenlund, Interactions between hadrons and nuclei: the Lund Monte Carlo – FRITIOF version 1.6. Comput. Phys. Commun. **43**, 387 (1987). https://doi.org/10.1016/0010-4655(87)90056-7. (**issn: 0010-4655**)
26. G. Folger, J. P. Wellisch, String Parton models in Geant4. (2003). https://doi.org/10.1088/1748-0221/12/12/P12009. arXiv:nucl-th/0306007
27. G. Folger, V.N. Ivanchenko, J.P. Wellisch, The binary cascade. Eur. Phys. J. A **21**, 407 (2004). https://doi.org/10.1088/1748-0221/12/12/P12009
28. ATLAS Collaboration, Study of the material of the ATLAS inner detector for Run 2 of the LHC. JINST **12**, P12009 (2017). https://doi.org/10.1088/1748-0221/12/12/P12009. arXiv:1707.02826 [hep-ex]
29. T. Sjöstrand et al., An introduction to PYTHIA 8.2. Comput. Phys. Commun. **191**, 159 (2015). https://doi.org/10.1016/j.cpc.2015.01.024. arXiv:1410.3012 [hep-ph]
30. ATLAS Collaboration, ATLAS Pythia 8 tunes to 7 TeV data. ATL-PHYS-PUB-2014-021 (2014). https://doi.org/10.1016/0550-3213(84)90607-2. https://cds.cern.ch/record/1966419
31. NNPDF Collaboration, R.D. Ball et al., Parton distributions with LHC data. Nucl. Phys. B **867**, 244 (2013). https://doi.org/10.1016/j.nuclphysb.2012.10.003. arXiv:1207.1303 [hep-ph]
32. T. Sjöstrand, Jet fragmentation of multiparton configurations in a string framework. Nucl. Phys. B **248**, 469 (1984). https://doi.org/10.1016/0550-3213(84)90607-2
33. B. Andersson, G. Gustafson, G. Ingelman, T. Sjöstrand, Parton fragmentation and string dynamics. Phys. Rep. **97**, 31 (1983). https://doi.org/10.1016/0370-1573(83)90080-7
34. D.J. Lange, The EvtGen particle decay simulation package. Nucl. Instrum. Methods A **462**, 152 (2001). https://doi.org/10.1016/S0168-9002(01)00089-4
35. E. Bothmann et al., Event generation with Sherpa 2.2. SciPost Phys. **7**, 034 (2019). https://doi.org/10.21468/SciPostPhys.7.3.034. arXiv:1905.09127 [hep-ph]
36. S. Dulat et al., New Parton distribution functions from a global analysis of quantum chromodynamics. Phys. Rev. D **93**, 033006 (2016). https://doi.org/10.1140/epjc/s2004-01960-8. arXiv:1506.07443 [hep-ph]
37. S. Schumann, F. Krauss, A Parton shower algorithm based on Catani–Seymour dipole factorisation. JHEP **03**, 038 (2008). https://doi.org/10.1088/1126-6708/2008/03/038. arXiv:0709.1027 [hep-ph]
38. J.-C. Winter, F. Krauss, G. Soff, A modified cluster-hadronisation model. Eur. Phys. J. C **36**, 381 (2004). https://doi.org/10.1140/epjc/s2004-01960-8. arXiv:hep-ph/0311085

39. G.S. Chahal, F. Krauss, Cluster hadronisation in Sherpa. SciPost Phys. **13**, 019 (2022). https://doi.org/10.21468/SciPostPhys.13.2.019. arXiv:2203.11385 [hep-ph]
40. T. Sjöstrand, S. Mrenna, P. Skands, A brief introduction to PYTHIA 8.1. Comput. Phys. Commun. **178**, 852 (2008). https://doi.org/10.1016/j.cpc.2008.01.036. arXiv:0710.3820 [hep-ph]
41. ATLAS Collaboration, The Pythia 8 A3 tune description of ATLAS minimum bias and inelastic measurements incorporating the Donnachie. Landshoff diffractive model. ATL-PHYS-PUB-2016-017 (2016). https://cds.cern.ch/record/2206965
42. ATLAS Collaboration, Electron and photon performance measurements with the ATLAS detector using the 2015-2017 LHC proton–proton collision data. JINST **14**, P12006 (2019). https://doi.org/10.1088/1748-0221/14/12/P12006. arXiv:1908.00005 [hep-ex]
43. ATLAS Collaboration, Electron and photon energy calibration with the ATLAS detector using LHC Run 2 data. JINST **19**, P02009 (2024). https://doi.org/10.1088/1748-0221/19/02/P02009. arXiv:2309.05471 [hep-ex]
44. M. Cacciari, G.P. Salam, Pileup subtraction using jet areas. Phys. Lett. B **659**, 119 (2008). https://doi.org/10.1016/j.physletb.2007.09.077. arXiv:0707.1378 [hep-ph]
45. ATLAS Collaboration, Studies of the muon momentum calibration and performance of the ATLAS detector with pp collisions at $\sqrt{s} = 13\,TeV$. Eur. Phys. J. C **83**, 686 (2023). https://doi.org/10.1140/epjc/s10052-023-11584-x. arXiv:2212.07338 [hep-ex]
46. ATLAS Collaboration, Alignment of the ATLAS inner detector in Run 2. Eur. Phys. J. C **80**, 1194 (2020). https://doi.org/10.1140/epjc/s10052-020-08700-6. arXiv:2007.07624 [hep-ex]
47. ATLAS Collaboration, Electron and photon energy calibration with the ATLAS detector using 2015–2016 LHC proton–proton collision data. JINST **14**, P03017 (2019). https://doi.org/10.1088/1748-0221/14/03/P03017. arXiv:1812.03848 [hep-ex]
48. J. Abdallah et al., Study of energy response and resolution of the ATLAS tile calorimeter to hadrons of energies from 16 to 30 GeV. Eur. Phys. J. C **81**, 549 (2021). https://doi.org/10.1140/epjc/s10052-021-09292-5. arXiv:2102.04088 [physics.ins-det]
49. P. Adragna et al., Measurement of pion and proton response and longitudinal shower profiles up to 20 nuclear interaction lengths with the ATLAS tile calorimeter. Nucl. Instrum. Methods A **615**, 158 (2010). https://doi.org/10.1016/j.nima.2010.01.037
50. P. Gras et al., Systematics of quark/gluon tagging. JHEP **07**, 091 (2017). https://doi.org/10.1007/JHEP07(2017)091. arXiv:1704.03878 [hep-ph]
51. P.T. Komiske, E.M. Metodiev, J. Thaler, An operational definition of quark and gluon jets. JHEP **11**, 059 (2018). https://doi.org/10.1007/JHEP11(2018)059. arXiv:1809.01140 [hep-ph]
52. ATLAS Collaboration, In situ calibration of large-radius jet energy and mass in 13 TeV proton–proton collisions with the ATLAS detector. Eur. Phys. J. C **79**, 135 (2019). https://doi.org/10.1140/epjc/s10052-019-6632-8. arXiv:1807.09477 [hep-ex]
53. Particle Data Group, P. Zyla et al., Review of particle physics. Prog. Theor. Exp. Phys. **2020**, 083C01 (2020). https://doi.org/10.1093/ptep/ptaa104
54. ATLAS Collaboration, Dependence of the jet energy scale on the particle content of hadronic jets in the ATLAS detector simulation. ATL-PHYS-PUB-2022-021 (2022). https://cds.cern.ch/record/2808016
55. ATLAS Collaboration, Measurements of jet cross-section ratios in 13 TeV proton–proton collisions with ATLAS. (2024). arXiv:2405.20206 [hep-ex]
56. T. Gleisberg et al., Event generation with SHERPA 1.1. JHEP **02**, 007 (2009). https://doi.org/10.1088/1126-6708/2009/02/007. arXiv:0811.4622 [hep-ph]
57. S. Höche, F. Krauss, S. Schumann, F. Siegert, QCD matrix elements and truncated showers. JHEP **05**, 053 (2009). https://doi.org/10.1088/1126-6708/2009/05/053. arXiv:0903.1219 [hep-ph]
58. B.R. Webber, A QCD model for jet fragmentation including soft gluon interference. Nucl. Phys. B **238**, 492 (1984). https://doi.org/10.1016/0550-3213(84)90333-X
59. G. Corcella et al., HERWIG 6: an event generator for hadron emission reactions with interfering gluons (including supersymmetric processes). JHEP **01**, 010 (2001). https://doi.org/10.1088/1126-6708/2001/01/010. arXiv:hep-ph/0011363
60. J. Bellm et al., Herwig 7.0/Herwig++ 3.0 release note. Eur. Phys. J. C **76**, 196 (2016). https://doi.org/10.1140/epjc/s10052-016-4018-8. arXiv:1512.01178 [hep-ph]
61. ATLAS Collaboration, Study of jet shapes in inclusive jet production in pp collisions at $\sqrt{s} = 7$ TeV using the ATLAS detector. Phys. Rev. D **83**, 052003 (2011). https://doi.org/10.1103/PhysRevD.83.052003. arXiv:1101.0070 [hep-ex]
62. ATLAS Collaboration, Properties of jet fragmentation using charged particles measured with the ATLAS detector in pp collisions at $\sqrt{s} = 13$ TeV. Phys. Rev. D **100**, 052011 (2019). https://doi.org/10.1103/PhysRevD.100.052011. arXiv:1906.09254 [hep-ex]
63. A.J. Larkoski, I. Moult, B. Nachman, Jet substructure at the large hadron collider: a review of recent advances in theory and machine learning. Phys. Rep. **841**, 1 (2020). https://doi.org/10.1016/j.physrep.2019.11.001. arXiv:1709.04464 [hep-ph]
64. R. Kogler et al., Jet substructure at the large hadron collider: experimental review. Rev. Mod. Phys. **91**, 045003 (2019). https://doi.org/10.1103/RevModPhys.91.045003. arXiv:1803.06991 [hep-ex]
65. ATLAS Collaboration, Optimisation of large-radius jet reconstruction for the ATLAS detector in 13 TeV proton–proton collisions. Eur. Phys. J. C **81**, 334 (2021). https://doi.org/10.1140/epjc/s10052-021-09054-3. arXiv:2009.04986 [hep-ex]
66. A.J. Larkoski, S. Marzani, G. Soyez, J. Thaler, Soft drop. JHEP **05**, 146 (2014). https://doi.org/10.1007/JHEP05(2014)146. arXiv:1402.2657 [hep-ph]
67. ATLAS Collaboration, ATLAS computing acknowledgements. ATL-SOFT-PUB-2025-001 (2025). https://cds.cern.ch/record/2922210

ATLAS Collaboration[⋆]

G. Aad[104], E. Aakvaag[17], B. Abbott[123], S. Abdelhameed[119a], K. Abeling[56], N. J. Abicht[50], S. H. Abidi[30], M. Aboelela[45], A. Aboulhorma[36e], H. Abramowicz[155], H. Abreu[154], Y. Abulaiti[120], B. S. Acharya[70a,70b,l], A. Ackermann[64a], C. Adam Bourdarios[4], L. Adamczyk[87a], S. V. Addepalli[27], M. J. Addison[103], J. Adelman[118], A. Adiguzel[22c], T. Adye[137], A. A. Affolder[139], Y. Afik[40], M. N. Agaras[13], J. Agarwala[74a,74b], A. Aggarwal[102], C. Agheorghiesei[28c], F. Ahmadov[39,aa], W. S. Ahmed[106], S. Ahuja[97], X. Ai[63e], G. Aielli[77a,77b], A. Aikot[166], M. Ait Tamlihat[36e], B. Aitbenchikh[36a], M. Akbiyik[102], T. P. A. Åkesson[100], A. V. Akimov[38], D. Akiyama[171], N. N. Akolkar[25], S. Aktas[22a], K. Al Khoury[42], G. L. Alberghi[24b], J. Albert[168], P. Albicocco[54], G. L. Albouy[61], S. Alderweireldt[53], Z. L. Alegria[124], M. Aleksa[37], I. N. Aleksandrov[39], C. Alexa[28b], T. Alexopoulos[10], F. Alfonsi[24b], M. Algren[57], M. Alhroob[170], B. Ali[135], H. M. J. Ali[93,t], S. Ali[32], S. W. Alibocus[94], M. Aliev[34c], G. Alimonti[72a], W. Alkakhi[56], C. Allaire[67], B. M. M. Allbrooke[150], J. S. Allen[103], J. F. Allen[53], C. A. Allendes Flores[140f], P. P. Allport[21], A. Aloisio[73a,73b], F. Alonso[92], C. Alpigiani[142], Z. M. K. Alsolami[93], M. Alvarez Estevez[101], A. Alvarez Fernandez[102], M. Alves Cardoso[57], M. G. Alviggi[73a,73b], M. Aly[103], Y. Amaral Coutinho[84b], A. Ambler[106], C. Amelung[37], M. Amerl[103], C. G. Ames[111], D. Amidei[108], B. Amini[55], K. Amirie[158], S. P. Amor Dos Santos[133a], K. R. Amos[166], D. Amperiadou[156], S. An[85], V. Ananiev[128], C. Anastopoulos[143], T. Andeen[11], J. K. Anders[37], A. C. Anderson[60], S. Y. Andrean[48a,48b], A. Andreazza[72a,72b], S. Angelidakis[9], A. Angerami[42], A. V. Anisenkov[38], A. Annovi[75a], C. Antel[57], E. Antipov[149], M. Antonelli[54], F. Anulli[76a], M. Aoki[85], T. Aoki[157], M. A. Aparo[150], L. Aperio Bella[49], C. Appelt[19], A. Apyan[27], S. J. Arbiol Val[88], C. Arcangeletti[54], A. T. H. Arce[52], J.-F. Arguin[110], S. Argyropoulos[55], J. -H. Arling[49], O. Arnaez[4], H. Arnold[149], G. Artoni[76a,76b], H. Asada[113], K. Asai[121], S. Asai[157], N. A. Asbah[37], R. A. Ashby Pickering[170], K. Assamagan[30], R. Astalos[29a], K. S. V. Astrand[100], S. Atashi[162], R. J. Atkin[34a], M. Atkinson[165], H. Atmani[36f], P. A. Atmasiddha[131], K. Augsten[135], S. Auricchio[73a,73b], A. D. Auriol[21], V. A. Austrup[103], G. Avolio[37], K. Axiotis[57], G. Azuelos[110,af], D. Babal[29b], H. Bachacou[138], K. Bachas[156,p], A. Bachiu[35], E. Bachmann[51], F. Backman[48a,48b], A. Badea[40], T. M. Baer[108], P. Bagnaia[76a,76b], M. Bahmani[19], D. Bahner[55], K. Bai[126], J. T. Baines[137], L. Baines[96], O. K. Baker[175], E. Bakos[16], D. Bakshi Gupta[8], L. E. Balabram Filho[84b], V. Balakrishnan[123], R. Balasubramanian[4], E. M. Baldin[38], P. Balek[87a], E. Ballabene[24a,24b], F. Balli[138], L. M. Baltes[64a], W. K. Balunas[33], J. Balz[102], I. Bamwidhi[119b], E. Banas[88], M. Bandieramonte[132], A. Bandyopadhyay[25], S. Bansal[25], L. Barak[155], M. Barakat[49], E. L. Barberio[107], D. Barberis[58a,58b], M. Barbero[104], M. Z. Barel[117], T. Barillari[112], M.-S. Barisits[37], T. Barklow[147], P. Baron[125], D. A. Baron Moreno[103], A. Baroncelli[63a], A. J. Barr[129], J. D. Barr[98], F. Barreiro[101], J. Barreiro Guimarães da Costa[14], U. Barron[155], M. G. Barros Teixeira[133a], S. Barsov[38], F. Bartels[64a], R. Bartoldus[147], A. E. Barton[93], P. Bartos[29a], A. Basan[102], M. Baselga[50], A. Bassalat[67,b], M. J. Basso[159a], S. Bataju[45], R. Bate[167], R. L. Bates[60], S. Batlamous[101], B. Batool[145], M. Battaglia[139], D. Battulga[19], M. Bauce[76a,76b], M. Bauer[80], P. Bauer[25], L. T. Bazzano Hurrell[31], J. B. Beacham[52], T. Beau[130], J. Y. Beaucamp[92], P. H. Beauchemin[161], P. Bechtle[25], H. P. Beck[20,o], K. Becker[170], A. J. Beddall[83], V. A. Bednyakov[39], C. P. Bee[149], L. J. Beemster[16], T. A. Beermann[37], M. Begalli[84d], M. Begel[30], A. Behera[149], J. K. Behr[49], J. F. Beirer[37], F. Beisiegel[25], M. Belfkir[119b], G. Bella[155], L. Bellagamba[24b], A. Bellerive[35], P. Bellos[21], K. Beloborodov[38], D. Benchekroun[36a], F. Bendebba[36a], Y. Benhammou[155], K. C. Benkendorfer[62], L. Beresford[49], M. Beretta[54], E. Bergeaas Kuutmann[164], N. Berger[4], B. Bergmann[135], J. Beringer[18a], G. Bernardi[5], C. Bernius[147], F. U. Bernlochner[25], F. Bernon[37], A. Berrocal Guardia[13], T. Berry[97], P. Berta[136], A. Berthold[51], S. Bethke[112], A. Betti[76a,76b], A. J. Bevan[96], N. K. Bhalla[55], S. Bhatta[149], D. S. Bhattacharya[169], P. Bhattarai[147], K. D. Bhide[55], V. S. Bhopatkar[124], R. M. Bianchi[132], G. Bianco[24a,24b], O. Biebel[111], R. Bielski[126], M. Biglietti[78a], C. S. Billingsley[45], Y. Bimgdi[36f], M. Bindi[56], A. Bingul[22b], C. Bini[76a,76b], G. A. Bird[33], M. Birman[172], M. Biros[136], S. Biryukov[150], T. Bisanz[50], E. Bisceglie[44a,44b], J. P. Biswal[137], D. Biswas[145], I. Bloch[49], A. Blue[60], U. Blumenschein[96], J. Blumenthal[102], V. S. Bobrovnikov[38], M. Boehler[55], B. Boehm[169], D. Bogavac[37], A. G. Bogdanchikov[38], L. S. Boggia[130], C. Bohm[48a], V. Boisvert[97], P. Bokan[37], T. Bold[87a], M. Bomben[5], M. Bona[96], M. Boonekamp[138], C. D. Booth[97], A. G. Borbély[60], I. S. Bordulev[38], G. Borissov[93], D. Bortoletto[129], D. Boscherini[24b], M. Bosman[13], J. D. Bossio Sola[37], K. Bouaouda[36a], N. Bouchhar[166], L. Boudet[4], J. Boudreau[132], E. V. Bouhova-Thacker[93], D. Boumediene[41], R. Bouquet[58a,58b], A. Boveia[122], J. Boyd[37], D. Boye[30], I. R. Boyko[39], L. Bozianu[57], J. Bracinik[21], N. Brahimi[4], G. Brandt[174], O. Brandt[33],

F. Braren[49], B. Brau[105], J. E. Brau[126], R. Brener[172], L. Brenner[117], R. Brenner[164], S. Bressler[172], G. Brianti[79a,79b], D. Britton[60], D. Britzger[112], I. Brock[25], R. Brock[109], G. Brooijmans[42], E. M. Brooks[159b], E. Brost[30], L. M. Brown[168], L. E. Bruce[62], T. L. Bruckler[129], P. A. Bruckman de Renstrom[88], B. Brüers[49], A. Bruni[24b], G. Bruni[24b], M. Bruschi[24b], N. Bruscino[76a,76b], T. Buanes[17], Q. Buat[142], D. Buchin[112], A. G. Buckley[60], O. Bulekov[38], B. A. Bullard[147], S. Burdin[94], C. D. Burgard[50], A. M. Burger[37], B. Burghgrave[8], O. Burlayenko[55], J. Burleson[165], J. T. P. Burr[33], J. C. Burzynski[146], E. L. Busch[42], V. Büscher[102], P. J. Bussey[60], J. M. Butler[26], C. M. Buttar[60], J. M. Butterworth[98], W. Buttinger[137], C. J. Buxo Vazquez[109], A. R. Buzykaev[38], S. Cabrera Urbán[166], L. Cadamuro[67], D. Caforio[59], H. Cai[132], Y. Cai[14,114c], Y. Cai[114a], V. M. M. Cairo[37], O. Cakir[3a], N. Calace[37], P. Calafiura[18a], G. Calderini[130], P. Calfayan[69], G. Callea[60], L. P. Caloba[84b], D. Calvet[41], S. Calvet[41], M. Calvetti[75a,75b], R. Camacho Toro[130], S. Camarda[37], D. Camarero Munoz[27], P. Camarri[77a,77b], M. T. Camerlingo[73a,73b], D. Cameron[37], C. Camincher[168], M. Campanelli[98], A. Camplani[43], V. Canale[73a,73b], A. C. Canbay[3a], E. Canonero[97], J. Cantero[166], Y. Cao[165], F. Capocasa[27], M. Capua[44a,44b], A. Carbone[72a,72b], R. Cardarelli[77a], J. C. J. Cardenas[8], G. Carducci[44a,44b], T. Carli[37], G. Carlino[73a], J. I. Carlotto[13], B. T. Carlson[132,q], E. M. Carlson[159a,168], J. Carmignani[94], L. Carminati[72a,72b], A. Carnelli[138], M. Carnesale[37], S. Caron[116], E. Carquin[140f], I.B. Carr[107], S. Carrá[72a], G. Carratta[24a,24b], A. M. Carroll[126], M. P. Casado[13,i], M. Caspar[49], F. L. Castillo[4], L. Castillo Garcia[13], V. Castillo Gimenez[166], N. F. Castro[133a,133e], A. Catinaccio[37], J. R. Catmore[128], T. Cavaliere[4], V. Cavaliere[30], N. Cavalli[24a,24b], L. J. Caviedes Betancourt[23b], Y. C. Cekmecelioglu[49], E. Celebi[83], S. Cella[37], M. S. Centonze[71a,71b], V. Cepaitis[57], K. Cerny[125], A. S. Cerqueira[84a], A. Cerri[150], L. Cerrito[77a,77b], F. Cerutti[18a], B. Cervato[145], A. Cervelli[24b], G. Cesarini[54], S. A. Cetin[83], D. Chakraborty[118], J. Chan[18a], W. Y. Chan[157], J. D. Chapman[33], E. Chapon[138], B. Chargeishvili[153b], D. G. Charlton[21], M. Chatterjee[20], C. Chauhan[136], Y. Che[114a], S. Chekanov[6], S. V. Chekulaev[159a], G. A. Chelkov[39,a], A. Chen[108], B. Chen[155], B. Chen[168], H. Chen[114a], H. Chen[30], J. Chen[63c], J. Chen[146], M. Chen[129], S. Chen[89], S. J. Chen[114a], X. Chen[63c], X. Chen[15,ae], Y. Chen[63a], C. L. Cheng[173], H. C. Cheng[65a], S. Cheong[147], A. Cheplakov[39], E. Cheremushkina[49], E. Cherepanova[117], R. Cherkaoui El Moursli[36e], E. Cheu[7], K. Cheung[66], L. Chevalier[138], V. Chiarella[54], G. Chiarelli[75a], N. Chiedde[104], G. Chiodini[71a], A. S. Chisholm[21], A. Chitan[28b], M. Chitishvili[166], M. V. Chizhov[39,r], K. Choi[11], Y. Chou[142], E. Y. S. Chow[116], K. L. Chu[172], M. C. Chu[65a], X. Chu[14,114c], Z. Chubinidze[54], J. Chudoba[134], J. J. Chwastowski[88], D. Cieri[112], K. M. Ciesla[87a], V. Cindro[95], A. Ciocio[18a], F. Cirotto[73a,73b], Z. H. Citron[172], M. Citterio[72a], D. A. Ciubotaru[28b], A. Clark[57], P. J. Clark[53], N. Clarke Hall[98], C. Clarry[158], J. M. Clavijo Columbie[49], S. E. Clawson[49], C. Clement[48a,48b], Y. Coadou[104], M. Cobal[70a,70c], A. Coccaro[58b], R. F. Coelho Barrue[133a], R. Coelho Lopes De Sa[105], S. Coelli[72a], B. Cole[42], J. Collot[61], P. Conde Muiño[133a,133g], M. P. Connell[34c], S. H. Connell[34c], E. I. Conroy[129], F. Conventi[73a,ag], H. G. Cooke[21], A. M. Cooper-Sarkar[129], F. A. Corchia[24a,24b], A. Cordeiro Oudot Choi[130], L. D. Corpe[41], M. Corradi[76a,76b], F. Corriveau[106,y], A. Cortes-Gonzalez[19], M. J. Costa[166], F. Costanza[4], D. Costanzo[143], B. M. Cote[122], J. Couthures[4], G. Cowan[97], K. Cranmer[173], L. Cremer[50], D. Cremonini[24a,24b], S. Crépé-Renaudin[61], F. Crescioli[130], M. Cristinziani[145], M. Cristoforetti[79a,79b], V. Croft[117], J. E. Crosby[124], G. Crosetti[44a,44b], A. Cueto[101], H. Cui[98], Z. Cui[7], W. R. Cunningham[60], F. Curcio[166], J. R. Curran[53], P. Czodrowski[37], M. J. Da Cunha Sargedas De Sousa[58a,58b], J. V. Da Fonseca Pinto[84b], C. Da Via[103], W. Dabrowski[87a], T. Dado[37], S. Dahbi[152], T. Dai[108], D. Dal Santo[20], C. Dallapiccola[105], M. Dam[43], G. D'amen[30], V. D'Amico[111], J. Damp[102], J. R. Dandoy[35], D. Dannheim[37], M. Danninger[146], V. Dao[149], G. Darbo[58b], S. J. Das[30], F. Dattola[49], S. D'Auria[72a,72b], A. D'Avanzo[73a,73b], C. David[34a], T. Davidek[136], I. Dawson[96], H. A. Day-hall[135], K. De[8], R. De Asmundis[73a], N. De Biase[49], S. De Castro[24a,24b], N. De Groot[116], P. de Jong[117], H. De la Torre[118], A. De Maria[114a], A. De Salvo[76a], U. De Sanctis[77a,77b], F. De Santis[71a,71b], A. De Santo[150], J. B. De Vivie De Regie[61], J. Debevc[95], D. V. Dedovich[39], J. Degens[94], A. M. Deiana[45], F. Del Corso[24a,24b], J. Del Peso[101], L. Delagrange[130], F. Deliot[138], C. M. Delitzsch[50], M. Della Pietra[73a,73b], D. Della Volpe[57], A. Dell'Acqua[37], L. Dell'Asta[72a,72b], M. Delmastro[4], P. A. Delsart[61], S. Demers[175], M. Demichev[39], S. P. Denisov[38], L. D'Eramo[41], D. Derendarz[88], F. Derue[130], P. Dervan[94], K. Desch[25], C. Deutsch[25], F. A. Di Bello[58a,58b], A. Di Ciaccio[77a,77b], L. Di Ciaccio[4], A. Di Domenico[76a,76b], C. Di Donato[73a,73b], A. Di Girolamo[37], G. Di Gregorio[37], A. Di Luca[79a,79b], B. Di Micco[78a,78b], R. Di Nardo[78a,78b], K. F. Di Petrillo[40], M. Diamantopoulou[35], F. A. Dias[117], T. Dias Do Vale[146], M. A. Diaz[140a,140b], F. G. Diaz Capriles[25], A. R. Didenko[39], M. Didenko[166], E. B. Diehl[108], S. Díez Cornell[49], C. Diez Pardos[145], C. Dimitriadi[164], A. Dimitrievska[21], J. Dingfelder[25], T. Dingley[129], I.-M. Dinu[28b],

S. J. Dittmeier[64b], F. Dittus[37], M. Divisek[136], B. Dixit[94], F. Djama[104], T. Djobava[153b], C. Doglioni[100,103], A. Dohnalova[29a], J. Dolejsi[136], Z. Dolezal[136], K. Domijan[87a], K. M. Dona[40], M. Donadelli[84d], B. Dong[109], J. Donini[41], A. D'Onofrio[73a,73b], M. D'Onofrio[94], J. Dopke[137], A. Doria[73a], N. Dos Santos Fernandes[133a], P. Dougan[103], M. T. Dova[92], A. T. Doyle[60], M. A. Draguet[129], M. P. Drescher[56], E. Dreyer[172], I. Drivas-koulouris[10], M. Drnevich[120], M. Drozdova[57], D. Du[63a], T. A. du Pree[117], F. Dubinin[38], M. Dubovsky[29a], E. Duchovni[172], G. Duckeck[111], O. A. Ducu[28b], D. Duda[53], A. Dudarev[37], E. R. Duden[27], M. D'uffizi[103], L. Duflot[67], M. Dührssen[37], I. Duminica[28g], A. E. Dumitriu[28b], M. Dunford[64a], S. Dungs[50], K. Dunne[48a,48b], A. Duperrin[104], H. Duran Yildiz[3a], M. Düren[59], A. Durglishvili[153b], D. Duvnjak[35], B. L. Dwyer[118], G. I. Dyckes[18a], M. Dyndal[87a], B. S. Dziedzic[37], Z. O. Earnshaw[150], G. H. Eberwein[129], B. Eckerova[29a], S. Eggebrecht[56], E. Egidio Purcino De Souza[84e], L. F. Ehrke[57], G. Eigen[17], K. Einsweiler[18a], T. Ekelof[164], P. A. Ekman[100], S. El Farkh[36b], Y. El Ghazali[63a], H. El Jarrari[37], A. El Moussaouy[36a], V. Ellajosyula[164], M. Ellert[164], F. Ellinghaus[174], N. Ellis[37], J. Elmsheuser[30], M. Elsawy[119a], M. Elsing[37], D. Emeliyanov[137], Y. Enari[85], I. Ene[18a], S. Epari[13], P. A. Erland[88], D. Ernani Martins Neto[88], M. Errenst[174], M. Escalier[67], C. Escobar[166], E. Etzion[155], G. Evans[133a,133b], H. Evans[69], L. S. Evans[97], A. Ezhilov[38], S. Ezzarqtouni[36a], F. Fabbri[24a,24b], L. Fabbri[24a,24b], G. Facini[98], V. Fadeyev[139], R. M. Fakhrutdinov[38], D. Fakoudis[102], S. Falciano[76a], L. F. Falda Ulhoa Coelho[37], F. Fallavollita[112], G. Falsetti[44a,44b], J. Faltova[136], C. Fan[165], K. Y. Fan[65b], Y. Fan[14], Y. Fang[14,114c], M. Fanti[72a,72b], M. Faraj[70a,70b], Z. Farazpay[99], A. Farbin[8], A. Farilla[78a], T. Farooque[109], S. M. Farrington[53], F. Fassi[36e], D. Fassouliotis[9], M. Faucci Giannelli[77a,77b], W. J. Fawcett[33], L. Fayard[67], P. Federic[136], P. Federicova[134], O. L. Fedin[38,a], M. Feickert[173], L. Feligioni[104], D. E. Fellers[126], C. Feng[63b], Z. Feng[117], M. J. Fenton[162], L. Ferencz[49], R. A. M. Ferguson[93], S. I. Fernandez Luengo[140f], P. Fernandez Martinez[68], M. J. V. Fernoux[104], J. Ferrando[93], A. Ferrari[164], P. Ferrari[116,117], R. Ferrari[74a], D. Ferrere[57], C. Ferretti[108], D. Fiacco[76a,76b], F. Fiedler[102], P. Fiedler[135], S. Filimonov[38], A. Filipčič[95], E. K. Filmer[159a], F. Filthaut[116], M. C. N. Fiolhais[133a,133c,c], L. Fiorini[166], W. C. Fisher[109], T. Fitschen[103], P. M. Fitzhugh[138], I. Fleck[145], P. Fleischmann[108], T. Flick[174], M. Flores[34d,ac], L. R. Flores Castillo[65a], L. Flores Sanz De Acedo[37], F. M. Follega[79a,79b], N. Fomin[33], J. H. Foo[158], A. Formica[138], A. C. Forti[103], E. Fortin[37], A. W. Fortman[18a], M. G. Foti[18a], L. Fountas[9,j], D. Fournier[67], H. Fox[93], P. Francavilla[75a,75b], S. Francescato[62], S. Franchellucci[57], M. Franchini[24a,24b], S. Franchino[64a], D. Francis[37], L. Franco[116], V. Franco Lima[37], L. Franconi[49], M. Franklin[62], G. Frattari[27], Y. Y. Frid[155], J. Friend[60], N. Fritzsche[37], A. Froch[55], D. Froidevaux[37], J. A. Frost[129], Y. Fu[63a], S. Fuenzalida Garrido[140f], M. Fujimoto[104], K. Y. Fung[65a], E. Furtado De Simas Filho[84e], M. Furukawa[157], J. Fuster[166], A. Gaa[56], A. Gabrielli[24a,24b], A. Gabrielli[158], P. Gadow[37], G. Gagliardi[58a,58b], L. G. Gagnon[18a], S. Gaid[163], S. Galantzan[155], J. Gallagher[1], E. J. Gallas[129], B. J. Gallop[137], K. K. Gan[122], S. Ganguly[157], Y. Gao[53], F. M. Garay Walls[140a,140b], B. Garcia[30], C. García[166], A. Garcia Alonso[117], A. G. Garcia Caffaro[175], J. E. García Navarro[166], M. Garcia-Scivetes[18a], G. L. Gardner[131], R. W. Gardner[40], N. Garelli[161], D. Garg[81], R. B. Garg[147], J. M. Gargan[53], C. A. Garner[158], C. M. Garvey[34a], V. K. Gassmann[161], G. Gaudio[74a], V. Gautam[13], P. Gauzzi[76a,76b], J. Gavranovic[95], I. L. Gavrilenko[38], A. Gavrilyuk[38], C. Gay[167], G. Gaycken[126], E. N. Gazis[10], A. A. Geanta[28b], C. M. Gee[139], A. Gekow[122], C. Gemme[58b], M. H. Genest[61], A. D. Gentry[115], S. George[97], W. F. George[21], T. Geralis[47], P. Gessinger-Befurt[37], M. E. Geyik[174], M. Ghani[170], K. Ghorbanian[96], A. Ghosal[145], A. Ghosh[162], A. Ghosh[7], B. Giacobbe[24b], S. Giagu[76a,76b], T. Giani[117], A. Giannini[63a], S. M. Gibson[97], M. Gignac[139], D. T. Gil[87b], A. K. Gilbert[87a], B. J. Gilbert[42], D. Gillberg[35], G. Gilles[117], L. Ginabat[130], D. M. Gingrich[2,af], M. P. Giordani[70a,70c], P. F. Giraud[138], G. Giugliarelli[70a,70c], D. Giugni[72a], F. Giuli[77a,77b], I. Gkialas[9,j], L. K. Gladilin[38], C. Glasman[101], G. R. Gledhill[126], G. Glemža[49], M. Glisic[126], I. Gnesi[44b], Y. Go[30], M. Goblirsch-Kolb[37], B. Gocke[50], D. Godin[110], B. Gokturk[22a], S. Goldfarb[107], T. Golling[57], M. G. D. Gololo[34g], D. Golubkov[38], J. P. Gombas[109], A. Gomes[133a,133b], G. Gomes Da Silva[145], A. J. Gomez Delegido[166], R. Gonçalo[133a], L. Gonella[21], A. Gongadze[153c], F. Gonnella[21], J. L. Gonski[147], R. Y. González Andana[53], S. González de la Hoz[166], R. Gonzalez Lopez[94], C. Gonzalez Renteria[18a], M. V. Gonzalez Rodrigues[49], R. Gonzalez Suarez[164], S. Gonzalez-Sevilla[57], L. Goossens[37], B. Gorini[37], E. Gorini[71a,71b], A. Gorišek[95], T. C. Gosart[131], A. T. Goshaw[52], M. I. Gostkin[39], S. Goswami[124], C. A. Gottardo[37], S. A. Gotz[111], M. Gouighri[36b], V. Goumarre[49], A. G. Goussiou[142], N. Govender[34c], R. P. Grabarczyk[129], I. Grabowska-Bold[87a], K. Graham[35], E. Gramstad[128], S. Grancagnolo[71a,71b], C. M. Grant[1,138], P. M. Gravila[28f], F. G. Gravili[71a,71b], H. M. Gray[18a], M. Greco[71a,71b], M. J. Green[1], C. Grefe[25], A. S. Grefsrud[17], I. M. Gregor[49], K. T. Greif[162], P. Grenier[147], S. G. Grewe[112], A. A. Grillo[139], K. Grimm[32], S. Grinstein[13,u], J. -F. Grivaz[67], E. Gross[172], J. Grosse-Knetter[56],

L. Guan[108], J. G. R. Guerrero Rojas[166], G. Guerrieri[37], R. Gugel[102], J. A. M. Guhit[108], A. Guida[19], E. Guilloton[170], S. Guindon[37], F. Guo[14,114c], J. Guo[63c], L. Guo[49], Y. Guo[108], A. Gupta[50], R. Gupta[132], S. Gurbuz[25], S. S. Gurdasani[55], G. Gustavino[76a,76b], P. Gutierrez[123], L. F. Gutierrez Zagazeta[131], M. Gutsche[51], C. Gutschow[98], C. Gwenlan[129], C. B. Gwilliam[94], E. S. Haaland[128], A. Haas[120], M. Habedank[60], C. Haber[18a], H. K. Hadavand[8], A. Hadef[51], S. Hadzic[112], A. I. Hagan[93], J. J. Hahn[145], E. H. Haines[98], M. Haleem[169], J. Haley[124], G. D. Hallewell[104], L. Halser[20], K. Hamano[168], M. Hamer[25], E. J. Hampshire[97], J. Han[63b], L. Han[114a], L. Han[63a], S. Han[18a], Y. F. Han[158], K. Hanagaki[85], M. Hance[139], D. A. Hangal[42], H. Hanif[146], M. D. Hank[131], J. B. Hansen[43], P. H. Hansen[43], D. Harada[57], T. Harenberg[174], S. Harkusha[38], M. L. Harris[105], Y. T. Harris[25], J. Harrison[13], N. M. Harrison[122], P. F. Harrison[170], N. M. Hartman[112], N. M. Hartmann[111], R. Z. Hasan[97,137], Y. Hasegawa[144], F. Haslbeck[129], S. Hassan[17], R. Hauser[109], C. M. Hawkes[21], R. J. Hawkings[37], Y. Hayashi[157], D. Hayden[109], C. Hayes[108], R. L. Hayes[117], C. P. Hays[129], J. M. Hays[96], H. S. Hayward[94], F. He[63a], M. He[14,114c], Y. He[49], Y. He[98], N. B. Heatley[96], V. Hedberg[100], A. L. Heggelund[128], N. D. Hehir[96,*], C. Heidegger[55], K. K. Heidegger[55], J. Heilman[35], S. Heim[49], T. Heim[18a], J. G. Heinlein[131], J. J. Heinrich[126], L. Heinrich[112,ad], J. Hejbal[134], A. Held[173], S. Hellesund[17], C. M. Helling[167], S. Hellman[48a,48b], R. C. W. Henderson[93], L. Henkelmann[33], A. M. Henriques Correia[37], H. Herde[100], Y. Hernández Jiménez[149], L. M. Herrmann[25], T. Herrmann[51], G. Herten[55], R. Hertenberger[111], L. Hervas[37], M. E. Hesping[102], N. P. Hessey[159a], J. Hessler[112], M. Hidaoui[36b], N. Hidic[136], E. Hill[158], S. J. Hillier[21], J. R. Hinds[109], F. Hinterkeuser[25], M. Hirose[127], S. Hirose[160], D. Hirschbuehl[174], T. G. Hitchings[103], B. Hiti[95], J. Hobbs[149], R. Hobincu[28e], N. Hod[172], M. C. Hodgkinson[143], B. H. Hodkinson[129], A. Hoecker[37], D. D. Hofer[108], J. Hofer[166], T. Holm[25], M. Holzbock[37], L. B. A. H. Hommels[33], B. P. Honan[103], J. J. Hong[69], J. Hong[63c], T. M. Hong[132], B. H. Hooberman[165], W. H. Hopkins[6], M. C. Hoppesch[165], Y. Horii[113], M. E. Horstmann[112], S. Hou[152], A. S. Howard[95], J. Howarth[60], J. Hoya[6], M. Hrabovsky[125], A. Hrynevich[49], T. Hryn'ova[4], P. J. Hsu[66], S. -C. Hsu[142], T. Hsu[67], M. Hu[18a], Q. Hu[63a], S. Huang[33], X. Huang[14,114c], Y. Huang[143], Y. Huang[102], Y. Huang[14], Z. Huang[103], Z. Hubacek[135], M. Huebner[25], F. Huegging[25], T. B. Huffman[129], M. Hufnagel Maranha De Faria[84a], C. A. Hugli[49], M. Huhtinen[37], S. K. Huiberts[17], R. Hulsken[106], N. Huseynov[12,g], J. Huston[109], J. Huth[62], R. Hyneman[147], G. Iacobucci[57], G. Iakovidis[30], L. Iconomidou-Fayard[67], J. P. Iddon[37], P. Iengo[73a,73b], R. Iguchi[157], Y. Iiyama[157], T. Iizawa[129], Y. Ikegami[85], N. Ilic[158], H. Imam[84c], G. Inacio Goncalves[84d], T. Ingebretsen Carlson[48a,48b], J. M. Inglis[96], G. Introzzi[74a,74b], M. Iodice[78a], V. Ippolito[76a,76b], R. K. Irwin[94], M. Ishino[157], W. Islam[173], C. Issever[19], S. Istin[22a,aj], H. Ito[171], R. Iuppa[79a,79b], A. Ivina[172], J. M. Izen[46], V. Izzo[73a], P. Jacka[134], P. Jackson[1], C. S. Jagfeld[111], G. Jain[159a], P. Jain[49], K. Jakobs[55], T. Jakoubek[172], J. Jamieson[60], W. Jang[157], M. Javurkova[105], P. Jawahar[103], L. Jeanty[126], J. Jejelava[153a,ab], P. Jenni[55,f], C. E. Jessiman[35], C. Jia[63b], H. Jia[167], J. Jia[149], X. Jia[14,114c], Z. Jia[114a], C. Jiang[53], S. Jiggins[49], J. Jimenez Pena[13], S. Jin[114a], A. Jinaru[28b], O. Jinnouchi[141], P. Johansson[143], K. A. Johns[7], J. W. Johnson[139], F. A. Jolly[49], D. M. Jones[150], E. Jones[49], K. S. Jones[8], P. Jones[33], R. W. L. Jones[93], T. J. Jones[94], H. L. Joos[37,56], R. Joshi[122], J. Jovicevic[16], X. Ju[18a], J. J. Junggeburth[105], T. Junkermann[64a], A. Juste Rozas[13,u], M. K. Juzek[88], S. Kabana[140e], A. Kaczmarska[88], M. Kado[112], H. Kagan[122], M. Kagan[147], A. Kahn[131], C. Kahra[102], T. Kaji[157], E. Kajomovitz[154], N. Kakati[172], I. Kalaitzidou[55], C. W. Kalderon[30], N. J. Kang[139], D. Kar[34g], K. Karava[129], M. J. Kareem[159b], E. Karentzos[55], O. Karkout[117], S. N. Karpov[39], Z. M. Karpova[39], V. Kartvelishvili[93], A. N. Karyukhin[38], E. Kasimi[156], J. Katzy[49], S. Kaur[35], K. Kawade[144], M. P. Kawale[123], C. Kawamoto[89], T. Kawamoto[63a], E. F. Kay[37], F. I. Kaya[161], S. Kazakos[109], V. F. Kazanin[38], Y. Ke[149], J. M. Keaveney[34a], R. Keeler[168], G. V. Kehris[62], J. S. Keller[35], J. J. Kempster[150], O. Kepka[134], B. P. Kerridge[137], S. Kersten[174], B. P. Kerševan[95], L. Keszeghova[29a], S. Ketabchi Haghighat[158], R. A. Khan[132], A. Khanov[124], A. G. Kharlamov[38], T. Kharlamova[38], E. E. Khoda[142], M. Kholodenko[133a], T. J. Khoo[19], G. Khoriauli[169], J. Khubua[153b,*], Y. A. R. Khwaira[130], B. Kibirige[34g], D. Kim[6], D. W. Kim[48a,48b], Y. K. Kim[40], N. Kimura[98], M. K. Kingston[56], A. Kirchhoff[56], C. Kirfel[25], F. Kirfel[25], J. Kirk[137], A. E. Kiryunin[112], S. Kita[160], C. Kitsaki[10], O. Kivernyk[25], M. Klassen[161], C. Klein[35], L. Klein[169], M. H. Klein[45], S. B. Klein[57], U. Klein[94], A. Klimentov[30], T. Klioutchnikova[37], P. Kluit[117], S. Kluth[112], E. Kneringer[80], T. M. Knight[158], A. Knue[50], M. Kobel[51], D. Kobylianskii[172], S. F. Koch[129], M. Kocian[147], P. Kodyš[136], D. M. Koeck[126], P. T. Koenig[25], T. Koffas[35], O. Kolay[51], I. Koletsou[4], T. Komarek[88], K. Köneke[55], A. X. Y. Kong[1], T. Kono[121], N. Konstantinidis[98], P. Kontaxakis[57], B. Konya[100], R. Kopeliansky[42], S. Koperny[87a], K. Korcyl[88], K. Kordas[156,e], A. Korn[98], S. Korn[56], I. Korolkov[13],

N. Korotkova[38], B. Kortman[117], O. Kortner[112], S. Kortner[112], W. H. Kostecka[118], V. V. Kostyukhin[145], A. Kotsokechagia[37], A. Kotwal[52], A. Koulouris[37], A. Kourkoumeli-Charalampidi[74a,74b], C. Kourkoumelis[9], E. Kourlitis[112], O. Kovanda[126], R. Kowalewski[168], W. Kozanecki[126], A. S. Kozhin[38], V. A. Kramarenko[38], G. Kramberger[95], P. Kramer[102], M. W. Krasny[130], A. Krasznahorkay[37], A. C. Kraus[118], J. W. Kraus[174], J. A. Kremer[49], T. Kresse[51], L. Kretschmann[174], J. Kretzschmar[94], K. Kreul[19], P. Krieger[158], M. Krivos[136], K. Krizka[21], K. Kroeninger[50], H. Kroha[112], J. Kroll[134], J. Kroll[131], K. S. Krowpman[109], U. Kruchonak[39], H. Krüger[25], N. Krumnack[82], M. C. Kruse[52], O. Kuchinskaia[38], S. Kuday[3a], S. Kuehn[37], R. Kuesters[55], T. Kuhl[49], V. Kukhtin[39], Y. Kulchitsky[38,a], S. Kuleshov[140b,140d], M. Kumar[34g], N. Kumari[49], P. Kumari[159b], A. Kupco[134], T. Kupfer[50], A. Kupich[38], O. Kuprash[55], H. Kurashige[86], L. L. Kurchaninov[159a], O. Kurdysh[67], Y. A. Kurochkin[38], A. Kurova[38], M. Kuze[141], A. K. Kvam[105], J. Kvita[125], T. Kwan[106], N. G. Kyriacou[108], L. A. O. Laatu[104], C. Lacasta[166], F. Lacava[76a,76b], H. Lacker[19], D. Lacour[130], N. N. Lad[98], E. Ladygin[39], A. Lafarge[41], B. Laforge[130], T. Lagouri[175], F. Z. Lahbabi[36a], S. Lai[56], J. E. Lambert[168], S. Lammers[69], W. Lampl[7], C. Lampoudis[156,e], G. Lamprinoudis[102], A. N. Lancaster[118], E. Lançon[30], U. Landgraf[55], M. P. J. Landon[96], V. S. Lang[55], O. K. B. Langrekken[128], A. J. Lankford[162], F. Lanni[37], K. Lantzsch[25], A. Lanza[74a], M. Lanzac Berrocal[166], J. F. Laporte[138], T. Lari[72a], F. Lasagni Manghi[24b], M. Lassnig[37], V. Latonova[134], A. Laurier[154], S. D. Lawlor[143], Z. Lawrence[103], R. Lazaridou[170], M. Lazzaroni[72a,72b], B. Le[103], H. D. M. Le[109], E. M. Le Boulicaut[175], L. T. Le Pottier[18a], B. Leban[24a,24b], A. Lebedev[82], M. LeBlanc[103], F. Ledroit-Guillon[61], S. C. Lee[152], S. Lee[48a,48b], T. F. Lee[94], L. L. Leeuw[34c], H. P. Lefebvre[97], M. Lefebvre[168], C. Leggett[18a], G. Lehmann Miotto[37], M. Leigh[57], W. A. Leight[105], W. Leinonen[116], A. Leisos[156,s], M. A. L. Leite[84c], C. E. Leitgeb[19], R. Leitner[136], K. J. C. Leney[45], T. Lenz[25], S. Leone[75a], C. Leonidopoulos[53], A. Leopold[148], R. Les[109], C. G. Lester[33], M. Levchenko[38], J. Levêque[4], L. J. Levinson[172], G. Levrini[24a,24b], M. P. Lewicki[88], C. Lewis[142], D. J. Lewis[4], L. Lewitt[143], A. Li[30], B. Li[63b], C. Li[63a], C.-Q. Li[112], H. Li[63a], H. Li[63b], H. Li[114a], H. Li[15], H. Li[63b], J. Li[63c], K. Li[14], L. Li[63c], M. Li[14,114c], S. Li[14,114c], S. Li[63c,63d,d], T. Li[5], X. Li[106], Z. Li[157], Z. Li[14,114c], Z. Li[63a], S. Liang[14,114c], Z. Liang[14], M. Liberatore[138], B. Liberti[77a], K. Lie[65c], J. Lieber Marin[84e], H. Lien[69], H. Lin[108], K. Lin[109], R. E. Lindley[7], J. H. Lindon[2], J. Ling[62], E. Lipeles[131], A. Lipniacka[17], A. Lister[167], J. D. Little[69], B. Liu[14], B. X. Liu[114b], D. Liu[63c,63d], E. H. L. Liu[21], J.B. Liu[63a], J. K. K. Liu[33], K. Liu[63d], K. Liu[63c,63d], M. Liu[63a], M. Y. Liu[63a], P. Liu[14], Q. Liu[63c,63d,142], X. Liu[63a], X. Liu[63b], Y. Liu[114b,114c], Y. L. Liu[63b], Y. W. Liu[63a], S. L. Lloyd[96], E. M. Lobodzinska[49], P. Loch[7], E. Lodhi[158], T. Lohse[19], K. Lohwasser[143], E. Loiacono[49], M. Lokajicek[134,*], J. D. Lomas[21], J. D. Long[42], I. Longarini[162], R. Longo[165], I. Lopez Paz[68], A. Lopez Solis[49], N. A. Lopez-canelas[7], N. Lorenzo Martinez[4], A. M. Lory[111], M. Losada[119a], G. Löschcke Centeno[150], O. Loseva[38], X. Lou[48a,48b], X. Lou[14,114c], A. Lounis[67], P. A. Love[93], G. Lu[14,114c], M. Lu[67], S. Lu[131], Y. J. Lu[66], H. J. Lubatti[142], C. Luci[76a,76b], F. L. Lucio Alves[114a], F. Luehring[69], O. Lukianchuk[67], B. S. Lunday[131], O. Lundberg[148], B. Lund-Jensen[148,*], N. A. Luongo[6], M. S. Lutz[37], A. B. Lux[26], D. Lynn[30], R. Lysak[134], E. Lytken[100], V. Lyubushkin[39], T. Lyubushkina[39], M. M. Lyukova[149], M. Firdaus M. Soberi[53], H. Ma[30], K. Ma[63a], L. L. Ma[63b], W. Ma[63a], Y. Ma[124], J. C. MacDonald[102], P. C. Machado De Abreu Farias[84e], R. Madar[41], T. Madula[98], J. Maeda[86], T. Maeno[30], H. Maguire[143], V. Maiboroda[138], A. Maio[133a,133b,133d], K. Maj[87a], O. Majersky[49], S. Majewski[126], N. Makovec[67], V. Maksimovic[16], B. Malaescu[130], Pa. Malecki[88], V. P. Maleev[38], F. Malek[61,n], M. Mali[95], D. Malito[97], U. Mallik[81,*], S. Maltezos[10], S. Malyukov[39], J. Mamuzic[13], G. Mancini[54], M. N. Mancini[27], G. Manco[74a,74b], J.P. Mandalia[96], S. S. Mandarry[150], I. Mandić[95], L. Manhaes de Andrade Filho[84a], I. M. Maniatis[172], J. Manjarres Ramos[91], D. C. Mankad[172], A. Mann[111], S. Manzoni[37], L. Mao[63c], X. Mapekula[34c], A. Marantis[156,s], G. Marchiori[5], M. Marcisovsky[134], C. Marcon[72a], M. Marinescu[21], S. Marium[49], M. Marjanovic[123], A. Markhoos[55], M. Markovitch[67], E. J. Marshall[93], Z. Marshall[18a], S. Marti-Garcia[166], J. Martin[98], T. A. Martin[137], V. J. Martin[53], B. Martin dit Latour[17], L. Martinelli[76a,76b], M. Martinez[13,u], P. Martinez Agullo[166], V. I. Martinez Outschoorn[105], P. Martinez Suarez[13], S. Martin-Haugh[137], G. Martinovicova[136], V. S. Martoiu[28b], A. C. Martyniuk[98], A. Marzin[37], D. Mascione[79a,79b], L. Masetti[102], J. Masik[103], A. L. Maslennikov[38], S. L. Mason[42], P. Massarotti[73a,73b], P. Mastrandrea[75a,75b], A. Mastroberardino[44a,44b], T. Masubuchi[127], T. T. Mathew[126], T. Mathisen[164], J. Matousek[136], D. M. Mattern[50], J. Maurer[28b], T. Maurin[60], A. J. Maury[67], B. Maček[95], D. A. Maximov[38], A. E. May[103], R. Mazini[152], I. Maznas[118], M. Mazza[109], S. M. Mazza[139], E. Mazzeo[72a,72b], C. Mc Ginn[30], J. P. Mc Gowan[168], S. P. Mc Kee[108], C. A. Mc Lean[6], C. C. McCracken[167], E. F. McDonald[107], A. E. McDougall[117], J. A. Mcfayden[150], R. P. McGovern[131],

R. P. Mckenzie[34g], T. C. Mclachlan[49], D. J. Mclaughlin[98], S. J. McMahon[137], C. M. Mcpartland[94], R. A. McPherson[168,y], S. Mehlhase[111], A. Mehta[94], D. Melini[166], B. R. Mellado Garcia[34g], A. H. Melo[56], F. Meloni[49], A. M. Mendes Jacques Da Costa[103], H. Y. Meng[158], L. Meng[93], S. Menke[112], M. Mentink[37], E. Meoni[44a,44b], G. Mercado[118], S. Merianos[156], C. Merlassino[70a,70c], L. Merola[73a,73b], C. Meroni[72a,72b], J. Metcalfe[6], A. S. Mete[6], E. Meuser[102], C. Meyer[69], J.-P. Meyer[138], R. P. Middleton[137], L. Mijović[53], G. Mikenberg[172], M. Mikestikova[134], M. Mikuž[95], H. Mildner[102], A. Milic[37], D. W. Miller[40], E. H. Miller[147], L. S. Miller[35], A. Milov[172], D. A. Milstead[48a,48b], T. Min[114a], A. A. Minaenko[38], I. A. Minashvili[153b], L. Mince[60], A. I. Mincer[120], B. Mindur[87a], M. Mineev[39], Y. Mino[89], L. M. Mir[13], M. Miralles Lopez[60], M. Mironova[18a], M. C. Missio[116], A. Mitra[170], V. A. Mitsou[166], Y. Mitsumori[113], O. Miu[158], P. S. Miyagawa[96], T. Mkrtchyan[64a], M. Mlinarevic[98], T. Mlinarevic[98], M. Mlynarikova[37], S. Mobius[20], P. Mogg[111], M. H. Mohamed Farook[115], A. F. Mohammed[14,114c], S. Mohapatra[42], G. Mokgatitswane[34g], L. Moleri[172], B. Mondal[145], S. Mondal[135], K. Mönig[49], E. Monnier[104], L. Monsonis Romero[166], J. Montejo Berlingen[13], A. Montella[48a,48b], M. Montella[122], F. Montereali[78a,78b], F. Monticelli[92], S. Monzani[70a,70c], A. Morancho Tarda[43], N. Morange[67], A. L. Moreira De Carvalho[49], M. Moreno Llácer[166], C. Moreno Martinez[57], J. M. Moreno Perez[23b], P. Morettini[58b], S. Morgenstern[37], M. Morii[62], M. Morinaga[157], M. Moritsu[90], F. Morodei[76a,76b], P. Moschovakos[37], B. Moser[129], M. Mosidze[153b], T. Moskalets[45], P. Moskvitina[116], J. Moss[32,k], P. Moszkowicz[87a], A. Moussa[36d], E. J. W. Moyse[105], O. Mtintsilana[34g], S. Muanza[104], J. Mueller[132], D. Muenstermann[93], R. Müller[37], G. A. Mullier[164], A. J. Mullin[33], J. J. Mullin[131], A. E. Mulski[62], D. P. Mungo[158], D. Munoz Perez[166], F. J. Munoz Sanchez[103], M. Murin[103], W. J. Murray[137,170], M. Muškinja[95], C. Mwewa[30], A. G. Myagkov[38,a], A. J. Myers[8], G. Myers[108], M. Myska[135], B. P. Nachman[18a], O. Nackenhorst[50], K. Nagai[129], K. Nagano[85], R. Nagasaka[157], J. L. Nagle[30,ah], E. Nagy[104], A. M. Nairz[37], Y. Nakahama[85], K. Nakamura[85], K. Nakkalil[5], H. Nanjo[127], E. A. Narayanan[45], I. Naryshkin[38], L. Nasella[72a,72b], M. Naseri[35], S. Nasri[119b], C. Nass[25], G. Navarro[23a], J. Navarro-Gonzalez[166], R. Nayak[155], A. Nayaz[19], P. Y. Nechaeva[38], S. Nechaeva[24a,24b], F. Nechansky[134], L. Nedic[129], T. J. Neep[21], A. Negri[74a,74b], M. Negrini[24b], C. Nellist[117], C. Nelson[106], K. Nelson[108], S. Nemecek[134], M. Nessi[37,h], M. S. Neubauer[165], F. Neuhaus[102], J. Neundorf[49], J. Newell[94], P. R. Newman[21], C. W. Ng[132], Y. W. Y. Ng[49], B. Ngair[119a], H. D. N. Nguyen[110], R. B. Nickerson[129], R. Nicolaidou[138], J. Nielsen[139], M. Niemeyer[56], J. Niermann[56], N. Nikiforou[37], V. Nikolaenko[38,a], I. Nikolic-Audit[130], K. Nikolopoulos[21], P. Nilsson[30], I. Ninca[49], G. Ninio[155], A. Nisati[76a], N. Nishu[2], R. Nisius[112], N. Nitika[70a,70c], J.-E. Nitschke[51], E. K. Nkadimeng[34g], T. Nobe[157], T. Nommensen[151], M. B. Norfolk[143], B. J. Norman[35], M. Noury[36a], J. Novak[95], T. Novak[95], L. Novotny[135], R. Novotny[115], L. Nozka[125], K. Ntekas[162], N. M. J. Nunes De Moura Junior[84b], J. Ocariz[130], A. Ochi[86], I. Ochoa[133a], S. Oerdek[49,v], J. T. Offermann[40], A. Ogrodnik[136], A. Oh[103], C. C. Ohm[148], H. Oide[85], R. Oishi[157], M. L. Ojeda[37], Y. Okumura[157], L. F. Oleiro Seabra[133a], I. Oleksiyuk[57], S. A. Olivares Pino[140d], G. Oliveira Correa[13], D. Oliveira Damazio[30], J. L. Oliver[162], Ö. O. Öncel[55], A. P. O'Neill[20], A. Onofre[133a,133e], P. U. E. Onyisi[11], M. J. Oreglia[40], G. E. Orellana[92], D. Orestano[78a,78b], N. Orlando[13], R. S. Orr[158], L. M. Osojnak[131], R. Ospanov[63a], Y. Osumi[113], G. Otero y Garzon[31], H. Otono[90], P. S. Ott[64a], G. J. Ottino[18a], M. Ouchrif[36d], F. Ould-Saada[128], T. Ovsiannikova[142], M. Owen[60], R. E. Owen[137], V. E. Ozcan[22a], F. Ozturk[88], N. Ozturk[8], S. Ozturk[83], H. A. Pacey[129], A. Pacheco Pages[13], C. Padilla Aranda[13], G. Padovano[76a,76b], S. Pagan Griso[18a], G. Palacino[69], A. Palazzo[71a,71b], J. Pampel[25], J. Pan[175], T. Pan[65a], D. K. Panchal[11], C. E. Pandini[117], J. G. Panduro Vazquez[137], H. D. Pandya[1], H. Pang[15], P. Pani[49], G. Panizzo[70a,70c], L. Panwar[130], L. Paolozzi[57], S. Parajuli[165], A. Paramonov[6], C. Paraskevopoulos[54], D. Paredes Hernandez[65b], A. Pareti[74a,74b], K. R. Park[42], T. H. Park[158], M. A. Parker[33], F. Parodi[58a,58b], E. W. Parrish[118], V. A. Parrish[53], J. A. Parsons[42], U. Parzefall[55], B. Pascual Dias[110], L. Pascual Dominguez[101], E. Pasqualucci[76a], S. Passaggio[58b], F. Pastore[97], P. Patel[88], U. M. Patel[52], J. R. Pater[103], T. Pauly[37], F. Pauwels[136], C. I. Pazos[161], M. Pedersen[128], R. Pedro[133a], S. V. Peleganchuk[38], O. Penc[37], E. A. Pender[53], S. Peng[15], G. D. Penn[175], K. E. Penski[111], M. Penzin[38], B. S. Peralva[84d], A. P. Pereira Peixoto[142], L. Pereira Sanchez[147], D. V. Perepelitsa[30,ah], G. Perera[105], E. Perez Codina[159a], M. Perganti[10], H. Pernegger[37], S. Perrella[76a,76b], O. Perrin[41], K. Peters[49], R. F. Y. Peters[103], B. A. Petersen[37], T. C. Petersen[43], E. Petit[104], V. Petousis[135], C. Petridou[156,e], T. Petru[136], A. Petrukhin[145], M. Pettee[18a], A. Petukhov[38], K. Petukhova[37], R. Pezoa[140f], L. Pezzotti[37], G. Pezzullo[175], A. J. Pfleger[37], T. M. Pham[173], T. Pham[107], P. W. Phillips[137], G. Piacquadio[149], E. Pianori[18a], F. Piazza[126], R. Piegaia[31], D. Pietreanu[28b], A. D. Pilkington[103], M. Pinamonti[70a,70c], J. L. Pinfold[2],

B. C. Pinheiro Pereira[133a], J. Pinol Bel[13], A. E. Pinto Pinoargote[138], L. Pintucci[70a,70c], K. M. Piper[150], A. Pirttikoski[57], D. A. Pizzi[35], L. Pizzimento[65b], A. Pizzini[117], M. -A. Pleier[30], V. Pleskot[136], E. Plotnikova[39], G. Poddar[96], R. Poettgen[100], L. Poggioli[130], I. Pokharel[56], S. Polacek[136], G. Polesello[74a], A. Poley[146,159a], A. Polini[24b], C. S. Pollard[170], Z. B. Pollock[122], E. Pompa Pacchi[76a,76b], N. I. Pond[98], D. Ponomarenko[69], L. Pontecorvo[37], S. Popa[28a], G. A. Popeneciu[28d], A. Poreba[37], D. M. Portillo Quintero[159a], S. Pospisil[135], M. A. Postill[143], P. Postolache[28c], K. Potamianos[170], P. A. Potepa[87a], I. N. Potrap[39], C. J. Potter[33], H. Potti[151], J. Poveda[166], M. E. Pozo Astigarraga[37], A. Prades Ibanez[77a,77b], J. Pretel[168], D. Price[103], M. Primavera[71a], L. Primomo[70a,70c], M. A. Principe Martin[101], R. Privara[125], T. Procter[60], M. L. Proffitt[142], N. Proklova[131], K. Prokofiev[65c], G. Proto[112], J. Proudfoot[6], M. Przybycien[87a], W. W. Przygoda[87b], A. Psallidas[47], J. E. Puddefoot[143], D. Pudzha[55], D. Pyatiizbyantseva[38], J. Qian[108], D. Qichen[103], Y. Qin[13], T. Qiu[53], A. Quadt[56], M. Queitsch-Maitland[103], G. Quetant[57], R. P. Quinn[167], G. Rabanal Bolanos[62], D. Rafanoharana[55], F. Raffaeli[77a,77b], F. Ragusa[72a,72b], J. L. Rainbolt[40], J. A. Raine[57], S. Rajagopalan[30], E. Ramakoti[38], L. Rambelli[58a,58b], I. A. Ramirez-Berend[35], K. Ran[49,114c], D. S. Rankin[131], N. P. Rapheeha[34g], H. Rasheed[28b], V. Raskina[130], D. F. Rassloff[64a], A. Rastogi[18a], S. Rave[102], S. Ravera[58a,58b], B. Ravina[56], I. Ravinovich[172], M. Raymond[37], A. L. Read[128], N. P. Readioff[143], D. M. Rebuzzi[74a,74b], G. Redlinger[30], A. S. Reed[112], K. Reeves[27], J. A. Reidelsturz[174], D. Reikher[126], A. Rej[50], C. Rembser[37], M. Renda[28b], F. Renner[49], A. G. Rennie[162], A. L. Rescia[49], S. Resconi[72a], M. Ressegotti[58a,58b], S. Rettie[37], J. G. Reyes Rivera[109], E. Reynolds[18a], O. L. Rezanova[38], P. Reznicek[136], H. Riani[36d], N. Ribaric[52], E. Ricci[79a,79b], R. Richter[112], S. Richter[48a,48b], E. Richter-Was[87b], M. Ridel[130], S. Ridouani[36d], P. Rieck[120], P. Riedler[37], E. M. Riefel[48a,48b], J. O. Rieger[117], M. Rijssenbeek[149], M. Rimoldi[37], L. Rinaldi[24a,24b], P. Rincke[56], T. T. Rinn[30], M. P. Rinnagel[111], G. Ripellino[164], I. Riu[13], J. C. Rivera Vergara[168], F. Rizatdinova[124], E. Rizvi[96], B. R. Roberts[18a], S. S. Roberts[139], S. H. Robertson[106,y], D. Robinson[33], M. Robles Manzano[102], A. Robson[60], A. Rocchi[77a,77b], C. Roda[75a,75b], S. Rodriguez Bosca[37], Y. Rodriguez Garcia[23a], A. Rodriguez Rodriguez[55], A. M. Rodríguez Vera[118], S. Roe[37], J. T. Roemer[37], A. R. Roepe-Gier[139], O. Røhne[128], R. A. Rojas[105], C. P. A. Roland[130], J. Roloff[30], A. Romaniouk[80], E. Romano[74a,74b], M. Romano[24b], A. C. Romero Hernandez[165], N. Rompotis[94], L. Roos[130], S. Rosati[76a], B. J. Rosser[40], E. Rossi[129], E. Rossi[73a,73b], L. P. Rossi[62], L. Rossini[55], R. Rosten[122], M. Rotaru[28b], B. Rottler[55], C. Rougier[91], D. Rousseau[67], D. Rousso[49], A. Roy[165], S. Roy-Garand[158], A. Rozanov[104], Z. M. A. Rozario[60], Y. Rozen[154], A. Rubio Jimenez[166], A. J. Ruby[94], V. H. Ruelas Rivera[19], T. A. Ruggeri[1], A. Ruggiero[129], A. Ruiz-Martinez[166], A. Rummler[37], Z. Rurikova[55], N. A. Rusakovich[39], H. L. Russell[168], G. Russo[76a,76b], J. P. Rutherfoord[7], S. Rutherford Colmenares[33], M. Rybar[136], E. B. Rye[128], A. Ryzhov[45], J. A. Sabater Iglesias[57], H. F.-W. Sadrozinski[139], F. Safai Tehrani[76a], B. Safarzadeh Samani[137], S. Saha[1], M. Sahinsoy[83], A. Saibel[166], M. Saimpert[138], M. Saito[157], T. Saito[157], A. Sala[72a,72b], D. Salamani[37], A. Salnikov[147], J. Salt[166], A. Salvador Salas[155], D. Salvatore[44a,44b], F. Salvatore[150], A. Salzburger[37], D. Sammel[55], E. Sampson[93], D. Sampsonidis[156,e], D. Sampsonidou[126], J. Sánchez[166], V. Sanchez Sebastian[166], H. Sandaker[128], C. O. Sander[49], J. A. Sandesara[105], M. Sandhoff[174], C. Sandoval[23b], L. Sanfilippo[64a], D. P. C. Sankey[137], T. Sano[89], A. Sansoni[54], L. Santi[37,76b], C. Santoni[41], H. Santos[133a,133b], A. Santra[172], E. Sanzani[24a,24b], K. A. Saoucha[163], J. G. Saraiva[133a,133d], J. Sardain[7], O. Sasaki[85], K. Sato[160], C. Sauer[64b], E. Sauvan[4], P. Savard[158,af], R. Sawada[157], C. Sawyer[137], L. Sawyer[99], C. Sbarra[24b], A. Sbrizzi[24a,24b], T. Scanlon[98], J. Schaarschmidt[142], U. Schäfer[102], A. C. Schaffer[45,67], D. Schaile[111], R. D. Schamberger[149], C. Scharf[19], M. M. Schefer[20], V. A. Schegelsky[38], D. Scheirich[136], M. Schernau[162], C. Scheulen[56], C. Schiavi[58a,58b], M. Schioppa[44a,44b], B. Schlag[147], S. Schlenker[37], J. Schmeing[174], M. A. Schmidt[174], K. Schmieden[102], C. Schmitt[102], N. Schmitt[102], S. Schmitt[49], L. Schoeffel[138], A. Schoening[64b], P. G. Scholer[35], E. Schopf[129], M. Schott[25], J. Schovancova[37], S. Schramm[57], T. Schroer[57], H.-C. Schultz-Coulon[64a], M. Schumacher[55], B. A. Schumm[139], Ph. Schune[138], A. J. Schuy[142], H. R. Schwartz[139], A. Schwartzman[147], T. A. Schwarz[108], Ph. Schwemling[138], R. Schwienhorst[109], F. G. Sciacca[20], A. Sciandra[30], G. Sciolla[27], F. Scuri[75a], C. D. Sebastiani[94], K. Sedlaczek[118], S. C. Seidel[115], A. Seiden[139], B. D. Seidlitz[42], C. Seitz[49], J. M. Seixas[84b], G. Sekhniaidze[73a], L. Selem[61], N. Semprini-Cesari[24a,24b], D. Sengupta[57], V. Senthilkumar[166], L. Serin[67], M. Sessa[77a,77b], H. Severini[123], F. Sforza[58a,58b], A. Sfyrla[57], Q. Sha[14], E. Shabalina[56], A. H. Shah[33], R. Shaheen[148], J. D. Shahinian[131], D. Shaked Renous[172], L. Y. Shan[14], M. Shapiro[18a], A. Sharma[37], A. S. Sharma[167], P. Sharma[81], P. B. Shatalov[38], K. Shaw[150], S. M. Shaw[103], Q. Shen[63c], D. J. Sheppard[146], P. Sherwood[98], L. Shi[98], X. Shi[14], S. Shimizu[85], C. O. Shimmin[175], J. D. Shinner[97], I. P. J. Shipsey[129,*], S. Shirabe[90],

M. Shiyakova[39,w], M. J. Shochet[40], D. R. Shope[128], B. Shrestha[123], S. Shrestha[122,ai], I. Shreyber[38], M. J. Shroff[168], P. Sicho[134], A. M. Sickles[165], E. Sideras Haddad[34g], A. C. Sidley[117], A. Sidoti[24b], F. Siegert[51], Dj. Sijacki[16], F. Sili[92], J. M. Silva[53], I. Silva Ferreira[84b], M. V. Silva Oliveira[30], S. B. Silverstein[48a], S. Simion[67], R. Simoniello[37], E. L. Simpson[103], H. Simpson[150], L. R. Simpson[108], S. Simsek[83], S. Sindhu[56], P. Sinervo[158], S. Singh[158], S. Sinha[49], S. Sinha[103], M. Sioli[24a,24b], I. Siral[37], E. Sitnikova[49], J. Sjölin[48a,48b], A. Skaf[56], E. Skorda[21], P. Skubic[123], M. Slawinska[88], V. Smakhtin[172], B. H. Smart[137], S. Yu. Smirnov[38], Y. Smirnov[38], L. N. Smirnova[38,a], O. Smirnova[100], A. C. Smith[42], D. R. Smith[162], E. A. Smith[40], J. L. Smith[103], R. Smith[147], M. Smizanska[93], K. Smolek[135], A. A. Snesarev[38], H. L. Snoek[117], S. Snyder[30], R. Sobie[168,y], A. Soffer[155], C. A. Solans Sanchez[37], E. Yu. Soldatov[38], U. Soldevila[166], A. A. Solodkov[38], S. Solomon[27], A. Soloshenko[39], K. Solovieva[55], O. V. Solovyanov[41], P. Sommer[51], A. Sonay[13], W. Y. Song[159b], A. Sopczak[135], A. L. Sopio[53], F. Sopkova[29b], J. D. Sorenson[115], I. R. Sotarriva Alvarez[141], V. Sothilingam[64a], O. J. Soto Sandoval[140b,140c], S. Sottocornola[69], R. Soualah[163], Z. Soumaimi[36e], D. South[49], N. Soybelman[172], S. Spagnolo[71a,71b], M. Spalla[112], D. Sperlich[55], G. Spigo[37], B. Spisso[73a,73b], D. P. Spiteri[60], M. Spousta[136], E. J. Staats[35], R. Stamen[64a], A. Stampekis[21], E. Stanecka[88], W. Stanek-Maslouska[49], M. V. Stange[51], B. Stanislaus[18a], M. M. Stanitzki[49], B. Stapf[49], E. A. Starchenko[38], G. H. Stark[139], J. Stark[91], P. Staroba[134], P. Starovoitov[64a], S. Stärz[106], R. Staszewski[88], G. Stavropoulos[47], A. Stefl[37], P. Steinberg[30], B. Stelzer[146,159a], H. J. Stelzer[132], O. Stelzer-Chilton[159a], H. Stenzel[59], T. J. Stevenson[150], G. A. Stewart[37], J. R. Stewart[124], M. C. Stockton[37], G. Stoicea[28b], M. Stolarski[133a], S. Stonjek[112], A. Straessner[51], J. Strandberg[148], S. Strandberg[48a,48b], M. Stratmann[174], M. Strauss[123], T. Strebler[104], P. Strizenec[29b], R. Ströhmer[169], D. M. Strom[126], R. Stroynowski[45], A. Strubig[48a,48b], S. A. Stucci[30], B. Stugu[17], J. Stupak[123], N. A. Styles[49], D. Su[147], S. Su[63a], W. Su[63d], X. Su[63a], D. Suchy[29a], K. Sugizaki[157], V. V. Sulin[38], M. J. Sullivan[94], D. M. S. Sultan[129], L. Sultanaliyeva[38], S. Sultansoy[3b], T. Sumida[89], S. Sun[173], O. Sunneborn Gudnadottir[164], N. Sur[104], M. R. Sutton[150], H. Suzuki[160], M. Svatos[134], M. Swiatlowski[159a], T. Swirski[169], I. Sykora[29a], M. Sykora[136], T. Sykora[136], D. Ta[102], K. Tackmann[49,v], A. Taffard[162], R. Tafirout[159a], J. S. Tafoya Vargas[67], Y. Takubo[85], M. Talby[104], A. A. Talyshev[38], K. C. Tam[65b], N. M. Tamir[155], A. Tanaka[157], J. Tanaka[157], R. Tanaka[67], M. Tanasini[149], Z. Tao[167], S. Tapia Araya[140f], S. Tapprogge[102], A. Tarek Abouelfadl Mohamed[109], S. Tarem[154], K. Tariq[14], G. Tarna[28b], G. F. Tartarelli[72a], M. J. Tartarin[91], P. Tas[136], M. Tasevsky[134], E. Tassi[44a,44b], A. C. Tate[165], G. Tateno[157], Y. Tayalati[36e,x], G. N. Taylor[107], W. Taylor[159b], R. Teixeira De Lima[147], P. Teixeira-Dias[97], J. J. Teoh[158], K. Terashi[157], J. Terron[101], S. Terzo[13], M. Testa[54], R. J. Teuscher[158,y], A. Thaler[80], O. Theiner[57], T. Theveneaux-Pelzer[104], O. Thielmann[174], D. W. Thomas[97], J. P. Thomas[21], E. A. Thompson[18a], P. D. Thompson[21], E. Thomson[131], R. E. Thornberry[45], C. Tian[63a], Y. Tian[57], V. Tikhomirov[38,a], Yu. A. Tikhonov[38], S. Timoshenko[38], D. Timoshyn[136], E. X. L. Ting[1], P. Tipton[175], A. Tishelman-Charny[30], S. H. Tlou[34g], K. Todome[141], S. Todorova-Nova[136], S. Todt[51], L. Toffolin[70a,70c], M. Togawa[85], J. Tojo[90], S. Tokár[29a], K. Tokushuku[85], O. Toldaiev[69], M. Tomoto[85,113], L. Tompkins[147,m], K. W. Topolnicki[87b], E. Torrence[126], H. Torres[91], E. Torró Pastor[166], M. Toscani[31], C. Tosciri[40], M. Tost[11], D. R. Tovey[143], I. S. Trandafir[28b], T. Trefzger[169], A. Tricoli[30], I. M. Trigger[159a], S. Trincaz-Duvoid[130], D. A. Trischuk[27], B. Trocmé[61], A. Tropina[39], L. Truong[34c], M. Trzebinski[88], A. Trzupek[88], F. Tsai[149], M. Tsai[108], A. Tsiamis[156], P. V. Tsiareshka[38], S. Tsigaridas[159a], A. Tsirigotis[156,s], V. Tsiskaridze[158], E. G. Tskhadadze[153a], M. Tsopoulou[156], Y. Tsujikawa[89], I.I. Tsukerman[38], V. Tsulaia[18a], S. Tsuno[85], K. Tsuri[121], D. Tsybychev[149], Y. Tu[65b], A. Tudorache[28b], V. Tudorache[28b], A. N. Tuna[62], S. Turchikhin[58a,58b], I. Turk Cakir[3a], R. Turra[72a], T. Turtuvshin[39,z], P. M. Tuts[42], S. Tzamarias[156,e], E. Tzovara[102], F. Ukegawa[160], P. A. Ulloa Poblete[140b,140c], E. N. Umaka[30], G. Unal[37], A. Undrus[30], G. Unel[162], J. Urban[29b], P. Urrejola[140a], G. Usai[8], R. Ushioda[141], M. Usman[110], F. Ustuner[53], Z. Uysal[83], V. Vacek[135], B. Vachon[106], T. Vafeiadis[37], A. Vaitkus[98], C. Valderanis[111], E. Valdes Santurio[48a,48b], M. Valente[159a], S. Valentinetti[24a,24b], A. Valero[166], E. Valiente Moreno[166], A. Vallier[91], J. A. Valls Ferrer[166], D. R. Van Arneman[117], T. R. Van Daalen[142], A. Van Der Graaf[50], P. Van Gemmeren[6], M. Van Rijnbach[37], S. Van Stroud[98], I. Van Vulpen[117], P. Vana[136], M. Vanadia[77a,77b], U. M. Vande Voorde[148], W. Vandelli[37], E. R. Vandewall[124], D. Vannicola[155], L. Vannoli[54], R. Vari[76a], E. W. Varnes[7], C. Varni[18b], T. Varol[152], D. Varouchas[67], L. Varriale[166], K. E. Varvell[151], M. E. Vasile[28b], L. Vaslin[85], G. A. Vasquez[168], A. Vasyukov[39], L. M. Vaughan[124], R. Vavricka[102], T. Vazquez Schroeder[37], J. Veatch[32], V. Vecchio[103], M. J. Veen[105], I. Veliscek[30], L. M. Veloce[158], F. Veloso[133a,133c], S. Veneziano[76a], A. Ventura[71a,71b], S. Ventura Gonzalez[138], A. Verbytskyi[112], M. Verducci[75a,75b], C. Vergis[96], M. Verissimo De Araujo[84b],

W. Verkerke[117], J. C. Vermeulen[117], C. Vernieri[147], M. Vessella[105], M. C. Vetterli[146,af], A. Vgenopoulos[102], N. Viaux Maira[140f], T. Vickey[143], O. E. Vickey Boeriu[143], G. H. A. Viehhauser[129], L. Vigani[64b], M. Vigl[112], M. Villa[24a,24b], M. Villaplana Perez[166], E. M. Villhauer[53], E. Vilucchi[54], M. G. Vincter[35], A. Visibile[117], C. Vittori[37], I. Vivarelli[24a,24b], E. Voevodina[112], F. Vogel[111], J. C. Voigt[51], P. Vokac[135], Yu. Volkotrub[87b], E. Von Toerne[25], B. Vormwald[37], V. Vorobel[136], K. Vorobev[38], M. Vos[166], K. Voss[145], M. Vozak[117], L. Vozdecky[123], N. Vranjes[16], M. Vranjes Milosavljevic[16], M. Vreeswijk[117], N. K. Vu[63c,63d], R. Vuillermet[37], O. Vujinovic[102], I. Vukotic[40], I. K. Vyas[35], S. Wada[160], C. Wagner[147], J. M. Wagner[18a], W. Wagner[174], S. Wahdan[174], H. Wahlberg[92], C. H. Waits[123], J. Walder[137], R. Walker[111], W. Walkowiak[145], A. Wall[131], E. J. Wallin[100], T. Wamorkar[6], A. Z. Wang[139], C. Wang[102], C. Wang[11], H. Wang[18a], J. Wang[65c], P. Wang[98], R. Wang[62], R. Wang[6], S. M. Wang[152], S. Wang[63b], S. Wang[14], T. Wang[63a], W.T. Wang[81], W. Wang[14], X. Wang[114a], X. Wang[165], X. Wang[63c], Y. Wang[63d], Y. Wang[114a], Y. Wang[63a], Z. Wang[108], Z. Wang[52,63c,63d], Z. Wang[108], A. Warburton[106], R. J. Ward[21], N. Warrack[60], S. Waterhouse[97], A. T. Watson[21], H. Watson[53], M. F. Watson[21], E. Watton[60,137], G. Watts[142], B. M. Waugh[98], J. M. Webb[55], C. Weber[30], H. A. Weber[19], M. S. Weber[20], S. M. Weber[64a], C. Wei[63a], Y. Wei[55], A. R. Weidberg[129], E. J. Weik[120], J. Weingarten[50], C. Weiser[55], C. J. Wells[49], T. Wenaus[30], B. Wendland[50], T. Wengler[37], N. S. Wenke[112], N. Wermes[25], M. Wessels[64a], A. M. Wharton[93], A. S. White[62], A. White[8], M. J. White[1], D. Whiteson[162], L. Wickremasinghe[127], W. Wiedenmann[173], M. Wielers[137], C. Wiglesworth[43], D. J. Wilbern[123], H. G. Wilkens[37], J. J. H. Wilkinson[33], D. M. Williams[42], H. H. Williams[131], S. Williams[33], S. Willocq[105], B. J. Wilson[103], P. J. Windischhofer[40], F. I. Winkel[31], F. Winklmeier[126], B. T. Winter[55], J. K. Winter[103], M. Wittgen[147], M. Wobisch[99], T. Wojtkowski[61], Z. Wolffs[117], J. Wollrath[162], M. W. Wolter[88], H. Wolters[133a,133c], M. C. Wong[139], E. L. Woodward[42], S. D. Worm[49], B. K. Wosiek[88], K. W. Woźniak[88], S. Wozniewski[56], K. Wraight[60], C. Wu[21], M. Wu[114b], M. Wu[116], S. L. Wu[173], X. Wu[57], Y. Wu[63a], Z. Wu[4], J. Wuerzinger[112,ad], T. R. Wyatt[103], B. M. Wynne[53], S. Xella[43], L. Xia[114a], M. Xia[15], M. Xie[63a], S. Xin[14,114c], A. Xiong[126], J. Xiong[18a], D. Xu[14], H. Xu[63a], L. Xu[63a], R. Xu[131], T. Xu[108], Y. Xu[15], Z. Xu[53], Z. Xu[114a], B. Yabsley[151], S. Yacoob[34a], Y. Yamaguchi[85], E. Yamashita[157], H. Yamauchi[160], T. Yamazaki[18a], Y. Yamazaki[86], S. Yan[60], Z. Yan[105], H. J. Yang[63c,63d], H. T. Yang[63a], S. Yang[63a], T. Yang[65c], X. Yang[37], X. Yang[14], Y. Yang[45], Y. Yang[63a], Z. Yang[63a], W.-M. Yao[18a], H. Ye[114a], H. Ye[56], J. Ye[14], S. Ye[30], X. Ye[63a], Y. Yeh[98], I. Yeletskikh[39], B. Yeo[18b], M. R. Yexley[98], T. P. Yildirim[129], P. Yin[42], K. Yorita[171], S. Younas[28b], C. J. S. Young[37], C. Young[147], C. Yu[14,114c], Y. Yu[63a], J. Yuan[14,114c], M. Yuan[108], R. Yuan[63c,63d], L. Yue[98], M. Zaazoua[63a], B. Zabinski[88], E. Zaid[53], Z. K. Zak[88], T. Zakareishvili[166], S. Zambito[57], J. A. Zamora Saa[140b,140d], J. Zang[157], D. Zanzi[55], O. Zaplatilek[135], C. Zeitnitz[174], H. Zeng[14], J. C. Zeng[165], D. T. Zenger Jr[27], O. Zenin[38], T. Ženiš[29a], S. Zenz[96], S. Zerradi[36a], D. Zerwas[67], M. Zhai[14,114c], D. F. Zhang[143], J. Zhang[63b], J. Zhang[6], K. Zhang[14,114c], L. Zhang[63a], L. Zhang[114a], P. Zhang[14,114c], R. Zhang[173], S. Zhang[108], S. Zhang[91], T. Zhang[157], X. Zhang[63c], X. Zhang[63b], Y. Zhang[63c], Y. Zhang[98], Y. Zhang[114a], Z. Zhang[18a], Z. Zhang[63b], Z. Zhang[67], H. Zhao[142], T. Zhao[63b], Y. Zhao[139], Z. Zhao[63a], Z. Zhao[63a], A. Zhemchugov[39], J. Zheng[114a], K. Zheng[165], X. Zheng[63a], Z. Zheng[147], D. Zhong[165], B. Zhou[108], H. Zhou[7], N. Zhou[63c], Y. Zhou[15], Y. Zhou[114a], Y. Zhou[7], C. G. Zhu[63b], J. Zhu[108], X. Zhu[63d], Y. Zhu[63c], Y. Zhu[63a], X. Zhuang[14], K. Zhukov[69], N. I. Zimine[39], J. Zinsser[64b], M. Ziolkowski[145], L. Živković[16], A. Zoccoli[24a,24b], K. Zoch[62], T. G. Zorbas[143], O. Zormpa[47], W. Zou[42], L. Zwalinski[37]

[1] Department of Physics, University of Adelaide, Adelaide, Australia
[2] Department of Physics, University of Alberta, Edmonton, AB, Canada
[3] [(a)]Department of Physics, Ankara University, Ankara, Turkey; [(b)]Division of Physics, TOBB University of Economics and Technology, Ankara, Turkey
[4] LAPP, Université Savoie Mont Blanc, CNRS/IN2P3, Annecy, France
[5] APC, Université Paris Cité, CNRS/IN2P3, Paris, France
[6] High Energy Physics Division, Argonne National Laboratory, Argonne, IL, USA
[7] Department of Physics, University of Arizona, Tucson, AZ, USA
[8] Department of Physics, University of Texas at Arlington, Arlington, TX, USA
[9] Physics Department, National and Kapodistrian University of Athens, Athens, Greece
[10] Physics Department, National Technical University of Athens, Zografou, Greece
[11] Department of Physics, University of Texas at Austin, Austin, TX, USA

[12] Institute of Physics, Azerbaijan Academy of Sciences, Baku, Azerbaijan
[13] Institut de Física d'Altes Energies (IFAE), Barcelona Institute of Science and Technology, Barcelona, Spain
[14] Institute of High Energy Physics, Chinese Academy of Sciences, Beijing, China
[15] Physics Department, Tsinghua University, Beijing, China
[16] Institute of Physics, University of Belgrade, Belgrade, Serbia
[17] Department for Physics and Technology, University of Bergen, Bergen, Norway
[18] [(a)]Physics Division, Lawrence Berkeley National Laboratory, Berkeley, CA, USA; [(b)]University of California, Berkeley, CA, USA
[19] Institut für Physik, Humboldt Universität zu Berlin, Berlin, Germany
[20] Albert Einstein Center for Fundamental Physics and Laboratory for High Energy Physics, University of Bern, Bern, Switzerland
[21] School of Physics and Astronomy, University of Birmingham, Birmingham, UK
[22] [(a)]Department of Physics, Bogazici University, Istanbul, Turkey; [(b)]Department of Physics Engineering, Gaziantep University, Gaziantep, Turkey; [(c)]Department of Physics, Istanbul University, Istanbul, Turkey
[23] [(a)]Facultad de Ciencias y Centro de Investigaciónes, Universidad Antonio Nariño, Bogotá, Colombia; [(b)]Departamento de Física, Universidad Nacional de Colombia, Bogotá, Colombia
[24] [(a)]Dipartimento di Fisica e Astronomia A. Righi, Università di Bologna, Bologna, Italy; [(b)]INFN Sezione di Bologna, Bologna, Italy
[25] Physikalisches Institut, Universität Bonn, Bonn, Germany
[26] Department of Physics, Boston University, Boston, MA, USA
[27] Department of Physics, Brandeis University, Waltham, MA, USA
[28] [(a)]Transilvania University of Brasov, Brasov, Romania; [(b)]Horia Hulubei National Institute of Physics and Nuclear Engineering, Bucharest, Romania; [(c)]Department of Physics, Alexandru Ioan Cuza University of Iasi, Iasi, Romania; [(d)]National Institute for Research and Development of Isotopic and Molecular Technologies, Physics Department, Cluj-Napoca, Romania; [(e)]National University of Science and Technology Politechnica, Bucharest, Romania; [(f)]West University in Timisoara, Timisoara, Romania; [(g)]Faculty of Physics, University of Bucharest, Bucharest, Romania
[29] [(a)]Faculty of Mathematics, Physics and Informatics, Comenius University, Bratislava, Slovakia; [(b)]Department of Subnuclear Physics, Institute of Experimental Physics of the Slovak Academy of Sciences, Kosice, Slovak Republic
[30] Physics Department, Brookhaven National Laboratory, Upton, NY, USA
[31] Universidad de Buenos Aires, Facultad de Ciencias Exactas y Naturales, Departamento de Física, y CONICET, Instituto de Física de Buenos Aires (IFIBA), Buenos Aires, Argentina
[32] California State University, Long Beach, CA, USA
[33] Cavendish Laboratory, University of Cambridge, Cambridge, UK
[34] [(a)]Department of Physics, University of Cape Town, Cape Town, South Africa; [(b)]iThemba Labs, Cape Town, Western Cape, South Africa; [(c)]Department of Mechanical Engineering Science, University of Johannesburg, Johannesburg, South Africa; [(d)]National Institute of Physics, University of the Philippines Diliman (Philippines), Quezon City, Philippines; [(e)]Department of Physics, University of South Africa, Pretoria, South Africa; [(f)]University of Zululand, KwaDlangezwa, Ongoye, South Africa; [(g)]School of Physics, University of the Witwatersrand, Johannesburg, South Africa
[35] Department of Physics, Carleton University, Ottawa, ON, Canada
[36] [(a)]Faculté des Sciences Ain Chock, Université Hassan II de Casablanca, Casablanca, Morocco; [(b)]Faculté des Sciences, Université Ibn-Tofail, Kénitra, Morocco; [(c)]Faculté des Sciences Semlalia, Université Cadi Ayyad, LPHEA-Marrakech, Marrakech, Morocco; [(d)]LPMR, Faculté des Sciences, Université Mohamed Premier, Oujda, Morocco; [(e)]Faculté des sciences, Université Mohammed V, Rabat, Morocco; [(f)]Institute of Applied Physics, Mohammed VI Polytechnic University, Ben Guerir, Morocco
[37] CERN, Geneva, Switzerland
[38] Affiliated with an Institute Covered by a Cooperation Agreement with CERN, Geneva, Switzerland
[39] Affiliated with an International Laboratory Covered by a Cooperation Agreement with CERN, Geneva, Switzerland
[40] Enrico Fermi Institute, University of Chicago, Chicago, IL, USA
[41] LPC, Université Clermont Auvergne, CNRS/IN2P3, Clermont-Ferrand, France
[42] Nevis Laboratory, Columbia University, Irvington, NY, USA
[43] Niels Bohr Institute, University of Copenhagen, Copenhagen, Denmark

[44] [(a)]Dipartimento di Fisica, Università della Calabria, Rende, Italy; [(b)]INFN Gruppo Collegato di Cosenza, Laboratori Nazionali di Frascati, Frascati, Italy
[45] Physics Department, Southern Methodist University, Dallas, TX, USA
[46] Physics Department, University of Texas at Dallas, Richardson, TX, USA
[47] National Centre for Scientific Research "Demokritos", Agia Paraskevi, Greece
[48] [(a)]Department of Physics, Stockholm University, Stockholm, Sweden; [(b)]Oskar Klein Centre, Stockholm, Sweden
[49] Deutsches Elektronen-Synchrotron DESY, Hamburg and Zeuthen, Germany
[50] Fakultät Physik , Technische Universität Dortmund, Dortmund, Germany
[51] Institut für Kern- und Teilchenphysik, Technische Universität Dresden, Dresden, Germany
[52] Department of Physics, Duke University, Durham, NC, USA
[53] SUPA-School of Physics and Astronomy, University of Edinburgh, Edinburgh, UK
[54] INFN e Laboratori Nazionali di Frascati, Frascati, Italy
[55] Physikalisches Institut, Albert-Ludwigs-Universität Freiburg, Freiburg, Germany
[56] II. Physikalisches Institut, Georg-August-Universität Göttingen, Göttingen, Germany
[57] Département de Physique Nucléaire et Corpusculaire, Université de Genève, Geneva, Switzerland
[58] [(a)]Dipartimento di Fisica, Università di Genova, Genoa, Italy; [(b)]INFN Sezione di Genova, Genoa, Italy
[59] II. Physikalisches Institut, Justus-Liebig-Universität Giessen, Giessen, Germany
[60] SUPA-School of Physics and Astronomy, University of Glasgow, Glasgow, UK
[61] LPSC, Université Grenoble Alpes, CNRS/IN2P3, Grenoble INP, Grenoble, France
[62] Laboratory for Particle Physics and Cosmology, Harvard University, Cambridge, MA, USA
[63] [(a)]Department of Modern Physics and State Key Laboratory of Particle Detection and Electronics, University of Science and Technology of China, Hefei, China; [(b)]Institute of Frontier and Interdisciplinary Science and Key Laboratory of Particle Physics and Particle Irradiation (MOE), Shandong University, Qingdao, China; [(c)]School of Physics and Astronomy, Shanghai Jiao Tong University, Key Laboratory for Particle Astrophysics and Cosmology (MOE), SKLPPC, Shanghai, China; [(d)]Tsung-Dao Lee Institute, Shanghai, China; [(e)]School of Physics, Zhengzhou University, Zhengzhou, China
[64] [(a)]Kirchhoff-Institut für Physik, Ruprecht-Karls-Universität Heidelberg, Heidelberg, Germany; [(b)]Physikalisches Institut, Ruprecht-Karls-Universität Heidelberg, Heidelberg, Germany
[65] [(a)]Department of Physics, Chinese University of Hong Kong, Shatin, N.T., Hong Kong; [(b)]Department of Physics, University of Hong Kong, Pok Fu Lam, Hong Kong; [(c)]Department of Physics and Institute for Advanced Study, Hong Kong University of Science and Technology, Clear Water Bay, Kowloon, Hong Kong, China
[66] Department of Physics, National Tsing Hua University, Hsinchu, Taiwan
[67] IJCLab, Université Paris-Saclay, CNRS/IN2P3, 91405, Orsay, France
[68] Centro Nacional de Microelectrónica (IMB-CNM-CSIC), Barcelona, Spain
[69] Department of Physics, Indiana University, Bloomington, IN, USA
[70] [(a)]INFN Gruppo Collegato di Udine, Sezione di Trieste, Udine, Italy; [(b)]ICTP, Trieste, Italy; [(c)]Dipartimento Politecnico di Ingegneria e Architettura, Università di Udine, Udine, Italy
[71] [(a)]INFN Sezione di Lecce, Lecce, Italy; [(b)]Dipartimento di Matematica e Fisica, Università del Salento, Lecce, Italy
[72] [(a)]INFN Sezione di Milano, Milan, Italy; [(b)]Dipartimento di Fisica, Università di Milano, Milan, Italy
[73] [(a)]INFN Sezione di Napoli, Naples, Italy; [(b)]Dipartimento di Fisica, Università di Napoli, Naples, Italy
[74] [(a)]INFN Sezione di Pavia, Pavia, Italy; [(b)]Dipartimento di Fisica, Università di Pavia, Pavia, Italy
[75] [(a)]INFN Sezione di Pisa, Pisa, Italy; [(b)]Dipartimento di Fisica E. Fermi, Università di Pisa, Pisa, Italy
[76] [(a)]INFN Sezione di Roma, Rome, Italy; [(b)]Dipartimento di Fisica, Sapienza Università di Roma, Rome, Italy
[77] [(a)]INFN Sezione di Roma Tor Vergata, Rome, Italy; [(b)]Dipartimento di Fisica, Università di Roma Tor Vergata, Rome, Italy
[78] [(a)]INFN Sezione di Roma Tre, Rome, Italy; [(b)]Dipartimento di Matematica e Fisica, Università Roma Tre, Rome, Italy
[79] [(a)]INFN-TIFPA, Trento, Italy; [(b)]Università degli Studi di Trento, Trento, Italy
[80] Universität Innsbruck, Department of Astro and Particle Physics, Innsbruck, Austria
[81] University of Iowa, Iowa City, IA, USA
[82] Department of Physics and Astronomy, Iowa State University, Ames, IA, USA
[83] Istinye University, Sariyer, Istanbul, Turkey
[84] [(a)]Departamento de Engenharia Elétrica, Universidade Federal de Juiz de Fora (UFJF), Juiz de Fora,

Brazil; [b]Universidade Federal do Rio De Janeiro COPPE/EE/IF, Rio de Janeiro, Brazil; [c]Instituto de Física, Universidade de São Paulo, São Paulo, Brazil; [d]Rio de Janeiro State University, Rio de Janeiro, Brazil; [e]Federal University of Bahia, Bahia, Brazil
[85] KEK, High Energy Accelerator Research Organization, Tsukuba, Japan
[86] Graduate School of Science, Kobe University, Kobe, Japan
[87] [a]Faculty of Physics and Applied Computer Science, AGH University of Krakow, Krakow, Poland; [b]Marian Smoluchowski Institute of Physics, Jagiellonian University, Krakow, Poland
[88] Institute of Nuclear Physics Polish Academy of Sciences, Krakow, Poland
[89] Faculty of Science, Kyoto University, Kyoto, Japan
[90] Research Center for Advanced Particle Physics and Department of Physics, Kyushu University, Fukuoka , Japan
[91] L2IT, Université de Toulouse, CNRS/IN2P3, UPS, Toulouse, France
[92] Instituto de Física La Plata, Universidad Nacional de La Plata and CONICET, La Plata, Argentina
[93] Physics Department, Lancaster University, Lancaster, UK
[94] Oliver Lodge Laboratory, University of Liverpool, Liverpool, UK
[95] Department of Experimental Particle Physics, Jožef Stefan Institute and Department of Physics, University of Ljubljana, Ljubljana, Slovenia
[96] School of Physics and Astronomy, Queen Mary University of London, London, UK
[97] Department of Physics, Royal Holloway University of London, Egham, UK
[98] Department of Physics and Astronomy, University College London, London, UK
[99] Louisiana Tech University, Ruston, LA, USA
[100] Fysiska institutionen, Lunds universitet, Lund, Sweden
[101] Departamento de Física Teorica C-15 and CIAFF, Universidad Autónoma de Madrid, Madrid, Spain
[102] Institut für Physik, Universität Mainz, Mainz, Germany
[103] School of Physics and Astronomy, University of Manchester, Manchester, UK
[104] CPPM, Aix-Marseille Université, CNRS/IN2P3, Marseille, France
[105] Department of Physics, University of Massachusetts, Amherst, MA, USA
[106] Department of Physics, McGill University, Montreal, QC, Canada
[107] School of Physics, University of Melbourne, Melbourne, VIC, Australia
[108] Department of Physics, University of Michigan, Ann Arbor, MI, USA
[109] Department of Physics and Astronomy, Michigan State University, East Lansing, MI, USA
[110] Group of Particle Physics, University of Montreal, Montreal, QC, Canada
[111] Fakultät für Physik, Ludwig-Maximilians-Universität München, Munich, Germany
[112] Max-Planck-Institut für Physik (Werner-Heisenberg-Institut), Munich, Germany
[113] Graduate School of Science and Kobayashi-Maskawa Institute, Nagoya University, Nagoya, Japan
[114] [a]Department of Physics, Nanjing University, Nanjing, China; [b]School of Science, Shenzhen Campus of Sun Yat-sen University, Shenzhen, China; [c]University of Chinese Academy of Science (UCAS), Beijing, China
[115] Department of Physics and Astronomy, University of New Mexico, Albuquerque, NM, USA
[116] Institute for Mathematics, Astrophysics and Particle Physics, Radboud University/Nikhef, Nijmegen, The Netherlands
[117] Nikhef National Institute for Subatomic Physics and University of Amsterdam, Amsterdam, The Netherlands
[118] Department of Physics, Northern Illinois University, DeKalb, IL, USA
[119] [a]New York University Abu Dhabi, Abu Dhabi, United Arab Emirates; [b]United Arab Emirates University, Al Ain, United Arab Emirates
[120] Department of Physics, New York University, New York, NY, USA
[121] Ochanomizu University, Otsuka, Bunkyo-ku, Tokyo, Japan
[122] Ohio State University, Columbus, OH, USA
[123] Homer L. Dodge Department of Physics and Astronomy, University of Oklahoma, Norman, OK, USA
[124] Department of Physics, Oklahoma State University, Stillwater, OK, USA
[125] Palacký University, Joint Laboratory of Optics, Olomouc, Czech Republic
[126] Institute for Fundamental Science, University of Oregon, Eugene, OR, USA
[127] Graduate School of Science, Osaka University, Osaka, Japan
[128] Department of Physics, University of Oslo, Oslo, Norway
[129] Department of Physics, Oxford University, Oxford, UK
[130] LPNHE, Sorbonne Université, Université Paris Cité, CNRS/IN2P3, Paris, France

[131] Department of Physics, University of Pennsylvania, Philadelphia, PA, USA
[132] Department of Physics and Astronomy, University of Pittsburgh, Pittsburgh, PA, USA
[133] [(a)]Laboratório de Instrumentação e Física Experimental de Partículas - LIP, Lisbon, Portugal; [(b)]Departamento de Física, Faculdade de Ciências, Universidade de Lisboa, Lisbon, Portugal; [(c)]Departamento de Física, Universidade de Coimbra, Coimbra, Portugal; [(d)]Centro de Física Nuclear da Universidade de Lisboa, Lisbon, Portugal; [(e)]Departamento de Física, Escola de Ciências, Universidade do Minho, Braga, Portugal; [(f)]Departamento de Física Teórica y del Cosmos, Universidad de Granada, Granada, Spain; [(g)]Departamento de Fısica, Instituto Superior Técnico, Universidade de Lisboa, Lisbon, Portugal
[134] Institute of Physics of the Czech Academy of Sciences, Prague, Czech Republic
[135] Czech Technical University in Prague, Prague, Czech Republic
[136] Faculty of Mathematics and Physics, Charles University, Prague, Czech Republic
[137] Particle Physics Department, Rutherford Appleton Laboratory, Didcot, UK
[138] IRFU, CEA, Université Paris-Saclay, Gif-sur-Yvette, France
[139] Santa Cruz Institute for Particle Physics, University of California Santa Cruz, Santa Cruz, CA, USA
[140] [(a)]Departamento de Física, Pontificia Universidad Católica de Chile, Santiago, Chile; [(b)]Millennium Institute for Subatomic physics at high energy frontier (SAPHIR), Santiago, Chile; [(c)]Instituto de Investigación Multidisciplinario en Ciencia y Tecnología y Departamento de Física, Universidad de La Serena, La Serena, Chile; [(d)]Universidad Andres Bello, Department of Physics, Santiago, Chile; [(e)]Instituto de Alta Investigación, Universidad de Tarapacá, Arica, Chile; [(f)]Departamento de Física, Universidad Técnica Federico Santa María, Valparaíso, Chile
[141] Department of Physics, Institute of Science, Tokyo, Japan
[142] Department of Physics, University of Washington, Seattle, WA, USA
[143] Department of Physics and Astronomy, University of Sheffield, Sheffield, UK
[144] Department of Physics, Shinshu University, Nagano, Japan
[145] Department Physik, Universität Siegen, Siegen, Germany
[146] Department of Physics, Simon Fraser University, Burnaby, BC, Canada
[147] SLAC National Accelerator Laboratory, Stanford, CA, USA
[148] Department of Physics, Royal Institute of Technology, Stockholm, Sweden
[149] Departments of Physics and Astronomy, Stony Brook University, Stony Brook, NY, USA
[150] Department of Physics and Astronomy, University of Sussex, Brighton, UK
[151] School of Physics, University of Sydney, Sydney, Australia
[152] Institute of Physics, Academia Sinica, Taipei, Taiwan
[153] [(a)]E. Andronikashvili Institute of Physics, Iv. Javakhishvili Tbilisi State University, Tbilisi, Georgia; [(b)]High Energy Physics Institute, Tbilisi State University, Tbilisi, Georgia; [(c)]University of Georgia, Tbilisi, Georgia
[154] Department of Physics, Technion, Israel Institute of Technology, Haifa, Israel
[155] Raymond and Beverly Sackler School of Physics and Astronomy, Tel Aviv University, Tel Aviv, Israel
[156] Department of Physics, Aristotle University of Thessaloniki, Thessaloniki, Greece
[157] International Center for Elementary Particle Physics and Department of Physics, University of Tokyo, Tokyo, Japan
[158] Department of Physics, University of Toronto, Toronto, ON, Canada
[159] [(a)]TRIUMF, Vancouver, BC, Canada; [(b)]Department of Physics and Astronomy, York University, Toronto, ON, Canada
[160] Division of Physics and Tomonaga Center for the History of the Universe, Faculty of Pure and Applied Sciences, University of Tsukuba, Tsukuba, Japan
[161] Department of Physics and Astronomy, Tufts University, Medford, MA, USA
[162] Department of Physics and Astronomy, University of California Irvine, Irvine, CA, USA
[163] University of Sharjah, Sharjah, United Arab Emirates
[164] Department of Physics and Astronomy, University of Uppsala, Uppsala, Sweden
[165] Department of Physics, University of Illinois, Urbana, IL, USA
[166] Instituto de Física Corpuscular (IFIC), Centro Mixto Universidad de Valencia-CSIC, Valencia, Spain
[167] Department of Physics, University of British Columbia, Vancouver, BC, Canada
[168] Department of Physics and Astronomy, University of Victoria, Victoria, BC, Canada
[169] Fakultät für Physik und Astronomie, Julius-Maximilians-Universität Würzburg, Würzburg, Germany
[170] Department of Physics, University of Warwick, Coventry, UK
[171] Waseda University, Tokyo, Japan

[172] Department of Particle Physics and Astrophysics, Weizmann Institute of Science, Rehovot, Israel
[173] Department of Physics, University of Wisconsin, Madison, WI, USA
[174] Fakultät für Mathematik und Naturwissenschaften, Fachgruppe Physik, Bergische Universität Wuppertal, Wuppertal, Germany
[175] Department of Physics, Yale University, New Haven, CT, USA

[a] Also Affiliated with an Institute Covered by a Cooperation Agreement with CERN, Geneva, Switzerland
[b] Also at An-Najah National University, Nablus, Palestine
[c] Also at Borough of Manhattan Community College, City University of New York, New York, NY, USA
[d] Also at Center for High Energy Physics, Peking University, China
[e] Also at Center for Interdisciplinary Research and Innovation (CIRI-AUTH), Thessaloniki, Greece
[f] Also at CERN, Geneva, Switzerland
[g] Also at CMD-AC UNEC Research Center, Azerbaijan State University of Economics (UNEC), Baku, Azerbaijan
[h] Also at Département de Physique Nucléaire et Corpusculaire, Université de Genève, Geneva, Switzerland
[i] Also at Departament de Fisica de la Universitat Autonoma de Barcelona, Barcelona, Spain
[j] Also at Department of Financial and Management Engineering, University of the Aegean, Chios, Greece
[k] Also at Department of Physics, California State University, Sacramento, USA
[l] Also at Department of Physics, King's College London, London, UK
[m] Also at Department of Physics, Stanford University, Stanford, CA, USA
[n] Also at Department of Physics, Stellenbosch University, Stellenbosch, South Africa
[o] Also at Department of Physics, University of Fribourg, Fribourg, Switzerland
[p] Also at Department of Physics, University of Thessaly, Volos, Greece
[q] Also at Department of Physics, Westmont College, Santa Barbara, USA
[r] Also at Faculty of Physics, Sofia University, 'St. Kliment Ohridski', Sofia, Bulgaria
[s] Also at Hellenic Open University, Patras, Greece
[t] Also at Imam Mohammad Ibn Saud Islamic University, Riyadh, Saudi Arabia
[u] Also at Institucio Catalana de Recerca i Estudis Avancats, ICREA, Barcelona, Spain
[v] Also at Institut für Experimentalphysik, Universität Hamburg, Hamburg, Germany
[w] Also at Institute for Nuclear Research and Nuclear Energy (INRNE) of the Bulgarian Academy of Sciences, Sofia, Bulgaria
[x] Also at Institute of Applied Physics, Mohammed VI Polytechnic University, Ben Guerir, Morocco
[y] Also at Institute of Particle Physics (IPP), Toronto, Canada
[z] Also at Institute of Physics and Technology, Mongolian Academy of Sciences, Ulaanbaatar, Mongolia
[aa] Also at Institute of Physics, Azerbaijan Academy of Sciences, Baku, Azerbaijan
[ab] Also at Institute of Theoretical Physics, Ilia State University, Tbilisi, Georgia
[ac] Also at National Institute of Physics, University of the Philippines Diliman (Philippines), Philippines
[ad] Also at Technical University of Munich, Munich, Germany
[ae] Also at The Collaborative Innovation Center of Quantum Matter (CICQM), Beijing, China
[af] Also at TRIUMF, Vancouver, BC, Canada
[ag] Also at Università di Napoli Parthenope, Naples, Italy
[ah] Also at Department of Physics, University of Colorado Boulder, Boulder, CO, USA
[ai] Also at Washington College, Chestertown, MD, USA
[aj] Also at Yeditepe University, Physics Department, Istanbul, Turkey
* Deceased